Studies of Electromagnetic Transitions in N^{15} and O^{15}†

E. K. WARBURTON, J. W. OLNESS, AND D. E. ALBURGER
Brookhaven National Laboratory, Upton, New York
(Received 23 July 1965)

Electromagnetic transitions in N^{15} and O^{15} have been investigated following the population of the bound levels of these nuclei by $N^{14}+d$, $C^{14}+d$, $C^{13}+He^3$, and $O^{16}+He^3$ with bombarding energies from 1.9 to 6.7 MeV. Gamma-ray angular distributions and relative intensities were determined using a three-crystal pair spectrometer. Gamma-ray branching ratios in N^{15} were determined through measurements of proton-gamma coincidence spectra following the $N^{14}(d,p)N^{15*}$ and $C^{13}(He^3,p)N^{15*}$ reactions. The ratios of radiative width to total width for the unbound 10.45- and 10.81-MeV levels of N^{15} were obtained as $\Gamma_\gamma/\Gamma>0.7$ and $\Gamma_\gamma/\Gamma=0.55_{-0.15}^{+0.25}$, respectively. Gamma-ray branching ratios in N^{15} and O^{15} were determined from measurements of gamma-gamma coincidence spectra using $N^{14}+d$, $C^{14}+d$, and $O^{16}+He^3$. Evidence was found for an excitation energy for the sixth excited state of O^{15} of 7.284 ± 0.007 MeV, rather than 7.17 ± 0.05 MeV as previously reported. Singles gamma-ray spectra were measured from all four targets using a lithium-drifted germanium detector. In these measurements, gamma-ray cascades to the 5.3-MeV doublet of N^{15} were separated, and it was determined that all the bound levels of N^{15} and O^{15} except the N^{15} 5.270- and O^{15} 5.240-MeV levels have mean lifetimes less than 5×10^{-13} sec. An intermediate-image magnetic spectrometer was used to study the angular correlation of internal pairs for ten ground-state transitions in N^{15} and O^{15}. From this work it was determined that the N^{15} 8.57-MeV level has $J^\pi=\frac{3}{2}^+$, the N^{15} 9.06- and 10.07-MeV levels have $J^\pi=\frac{1}{2}^+$ or $\frac{3}{2}^+$, the 9.76- and 9.93-MeV levels are most probably $J^\pi=\frac{1}{2}^+$ or $\frac{3}{2}^+$, and the 9.16-MeV level is most probably $J^\pi=\frac{3}{2}^-$. For the remaining levels the measurements serve to restrict the range of possible spin-parity assignments. The correspondence between mirror levels in N^{15} and O^{15} is discussed and a comparison with theoretical predictions is made.

I. INTRODUCTION

THE measurements reported herein were performed to gain information on the bound energy levels of N^{15} and O^{15} and the gamma-ray transitions connecting them. The previously published information on the spin-parity assignments of these levels is illustrated in Fig. 1. Included in this figure are the known N^{15} levels below 11.2-MeV excitation and the known O^{15} levels below 11.7-MeV excitation. The references for the existence and energies of the levels are, with a few exceptions, the compilations of Ajzenberg-Selove and Lauritsen.[1,2] The excitation energies of the 5-MeV doublets in N^{15} are taken from the $N^{14}(n,\gamma)N^{15}$ results of Carter and Motz[3] and recent measurements with a lithium-drifted germanium (Li-Ge) detector.[4] The two levels at 9.77- and 9.94-MeV excitation in N^{15} were considered as doubtful by Lauritsen and Ajzenberg-Selove[2] because they had been observed only as slow-neutron thresholds in the $C^{14}(d,n)N^{15}$ reaction.[5] However, these two levels have since been observed in magnetic-spectrometer studies of the $N^{14}(d,p)N^{15}$ reaction[6,7] and the $C^{13}(He^3,p)N^{15}$ reaction[7] and so we consider these to be confirmed. Evidence for a level at

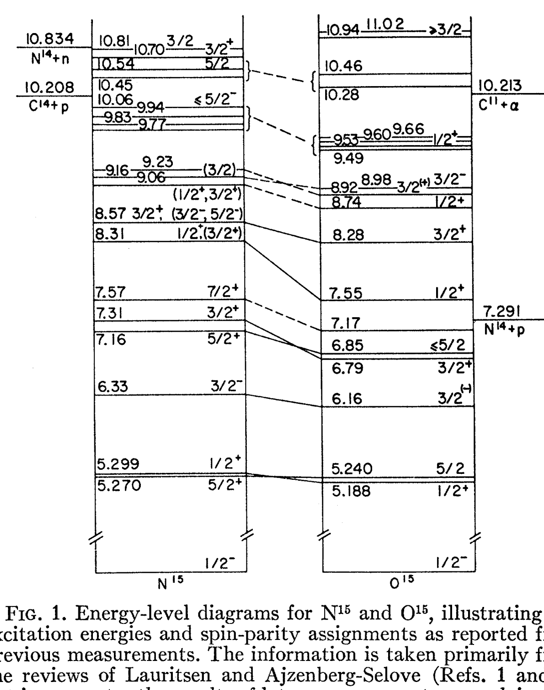

FIG. 1. Energy-level diagrams for N^{15} and O^{15}, illustrating the excitation energies and spin-parity assignments as reported from previous measurements. The information is taken primarily from the reviews of Lauritsen and Ajzenberg-Selove (Refs. 1 and 2) but incorporates the results of later measurements as explained in the text. Uncertain spin-parity assignments or less likely alternatives are enclosed in parentheses. Mirror levels in N^{15} and O^{15} are connected by solid lines if the correspondence is well established and by dashed lines if the correspondence is uncertain or speculative.

† Work performed under the auspices of the U. S. Atomic Energy Commission.

[1] F. Ajzenberg-Selove and T. Lauritsen, Nucl. Phys. **11**, 1 (1959).

[2] T. Lauritsen and F. Ajzenberg-Selove, *Nuclear Data Sheets*, compiled by K. Way *et al.* (Printing and Publishing Office, National Academy of Sciences–National Research Council, Washington 25, D. C., 1962), sets 5 and 6.

[3] R. E. Carter and H. T. Motz, *International Conference on Nuclear Physics with Reactor Neutrons*, edited by F. E. Throw, (Argonne National Laboratory, Argonne, Illinois, 1963), pp. 179–182; H. T. Motz, R. E. Carter, and W. D. Barfield, *Pile Neutron Research in Physics* (International Atomic Energy Agency, Vienna, 1962), pp. 225–238; H. T. Motz (private communication).

[4] E. K. Warburton, K. W. Jones, D. E. Alburger, C. Chasman, and R. A. Ristinen, Phys. Rev. Letters **14**, 146 (1965).

[5] R. Chiba, Phys. Rev. **123**, 1316 (1961).

[6] E. Kashy (private communication).

[7] A. Gallmann (private communication).

9.231 ± 0.008 MeV was also found in these studies.[6,7] The MIT group[6] also reported levels at excitation energies of 8.739 ± 0.008, 9.598 ± 0.010, and 8.643 ± 0.009 (doubtful) MeV; however, these levels are not included in Fig. 1 since they have not been confirmed by the Strasbourg group[7] in their magnetic spectrograph measurements on the $C^{13}(He^3,p)N^{15}$ and $N^{14}(d,p)N^{15}$ reactions.

We now consider the spin-parity assignments of Fig. 1—some of which are different from those given by Lauritsen and Ajzenberg-Selove.[2] The suspected $J^\pi=\frac{5}{2}+$ assignment to the first-excited state of N^{15} has recently been authenticated by gamma-ray angular distribution and correlation measurements.[8,9] Previously, this assignment was open to some question.[9] The N^{15} 5.299-MeV level is fixed as $J^\pi=\frac{1}{2}+$ or $\frac{3}{2}+$ by the C^{15} beta-decay branch to it.[10,11] An intense neutron group corresponding to the unresolved 5.3-MeV doublet of N^{15} with an angular distribution peaking strongly forward (i.e., $l_p=0$) is observed in the $C^{14}(d,n)N^{15}$ reaction at $E_d=3.53$ MeV[5] and 2.10 and 2.33 MeV.[12] The N^{15} 5.270-MeV level has $J^\pi=\frac{5}{2}+$ and thus should have an $l_p=2$ stripping pattern since the C^{14} ground state has[1,2] $J^\pi=0^+$; likewise if the 5.299-MeV level had $J^\pi=\frac{3}{2}+$ it should have an $l_p=2$ stripping pattern. These results thus show that the 5.299-MeV level has $J^\pi=\frac{1}{2}+$ and is formed more strongly in the $C^{14}(d,n)N^{15}$ reaction than is the 5.270-MeV level—at least at forward angles.[13]

The parity assignments for all the bound levels of N^{15} save the N^{15} 5.299-MeV level were determined by analysis of stripping reactions.[1,2] The spin assignment for the N^{15} 6.33-MeV level has recently been confirmed by gamma-ray correlation studies.[9] The spin assignments of the N^{15} 7.16- and 7.57-MeV levels have been obtained in a similar manner.[8]

The N^{15} 8.31-MeV level has $J^\pi=\frac{1}{2}+$ or $\frac{3}{2}+$ from stripping results.[1,2] The preference for $J^\pi=\frac{1}{2}+$ follows observation of isotropy for the gamma-ray transitions from this level in two angular correlation measurements.[8,9] The same measurements[8,9] rule out the possibility of $J=\frac{1}{2}$ for the 8.57-MeV level and demand[9] $J=\frac{3}{2}$ if the 8.31-MeV level has $J=\frac{1}{2}$. Analysis of $N^{14}(d,p)N^{15}$ stripping results favors a mixture of $l_n=0$ and $l_n=2$ and thus $J^\pi=\frac{3}{2}+$ for the N^{15} 8.57-MeV level[14,15]; however, $l_n=1$ and thus $J^\pi=\frac{3}{2}-$ or $\frac{5}{2}-$ cannot be completely excluded[16] and so remain as unfavored possibilities.

The N^{15} 9.06-MeV level is reported to be formed by $l_n=0$ neutron capture in the $N^{14}(d,p)N^{15}$ reaction while correspondingly no clear stripping pattern for the 9.16-MeV level is observed.[14] In contrast, Green and Middleton[16] obtain an $l_n=1$ pattern for the unresolved 9.06-, 9.16-MeV doublet. Thus, we give a doubtful $\frac{1}{2}+$ or $\frac{3}{2}+$ assignment to the 9.06-MeV level and no assignment to the 9.16-MeV level from this source.

The 9.16-MeV level decays[3] by gamma emission to the $J=\frac{1}{2}$ ground state and 5.299-MeV level and the $J=\frac{3}{2}$, 6.33- and $J=\frac{5}{2}$, 7.16-MeV levels. Because of these decay modes we give a preference for $J=\frac{3}{2}$ to this level. The range of possible assignments indicated for the N^{15} 10.06-MeV level follows from observation of an $l_n=1$ stripping pattern for this level in the $N^{14}(d,p)N^{15}$ reaction.[16]

The spin-parity assignments for the four N^{15} levels between the thresholds for proton and neutron emission follow the assignments of Hebbard and Dunbar[17] and Hebbard.[18]

The first-excited state of O^{15} at 5.188 MeV can be assigned $J^\pi=\frac{1}{2}+$ on the basis of the $O^{16}(He^3,\alpha)O^{15}$ pickup results of Hinds and Middleton.[19] This assignment is consistent with the $J=\frac{1}{2}$ or $\frac{3}{2}$ limitation set by Povh and Hebbard.[20]

The second-excited state of O^{15} at 5.240 MeV has recently been assigned $J=\frac{5}{2}$ on the basis of particle-gamma correlation measurements of its ground-state decay following the $O^{16}(He^3,\alpha)O^{15*}$ reaction.[7]

Povh and Hebbard[20] assigned $J=\frac{3}{2}$ to both the O^{15} 6.16- and 6.79-MeV levels. The 6.16-MeV level has been given a most probable assignment of odd parity since the ground-state transition from this level has a sizeable quadrupole contribution[20] which we interpret as being more probably an $M1$, $E2$ mixture rather than $E1$, $M2$. The 6.79-MeV level is given an even-parity assignment because the angular distribution of the gamma ray feeding it following nonresonant capture of protons by N^{14} have the nearly pure $\sin^2\theta$ dependence which is the signature of p-wave capture into an s state.[21,22]

The information on the parity assignments to the bound O^{15} levels from $N^{14}(d,n)O^{15}$ is quite scanty and for the most part inconclusive. A highly tentative

[8] D. Pelte, B. Povh, and W. Scholz, International Congress of Nuclear Physics, Paris, July 1964 (to be published); and B. Povh (private communication).

[9] E. K. Warburton, J. S. Lopes, R. W. Ollerhead, A. R. Poletti, and M. F. Thomas, Phys. Rev. **138**, B104 (1965).

[10] D. E. Alburger, A. Gallmann, and D. H. Wilkinson, Phys. Rev. **116**, 939 (1959).

[11] D. E. Alburger, C. Chasman, K. W. Jones, and R. A. Ristinen, Phys. Rev. **136**, B913 (1964).

[12] W. L. Imhof, H. W. Grench, and R. G. Johnson, Nucl. Phys. **49**, 503 (1963).

[13] The $C^{14}(d,n)N^{15}$ measurements (Refs. 5 and 12) were overlooked in recent work on the 5.3-MeV doublet of N^{15} (Ref. 9) so that $J^\pi=\frac{3}{2}+$ for the 5.299-MeV level was retained as a possibility in the report of that work.

[14] R. D. Sharp, A. Sperduto, and W. W. Buechner, Phys. Rev. **99**, 632 (1955); Massachusetts Institute of Technology Laboratory for Nuclear Science Progress Report, May 1955 (unpublished).

[15] E. K. Warburton and J. N. McGruer, Phys. Rev. **105**, 639 (1957).

[16] T. S. Green and R. Middleton, Proc. Phys. Soc. (London) **A69**, 28 (1955).

[17] D. F. Hebbard and D. N. F. Dunbar, Phys. Rev. **115**, 624 (1958).

[18] D. F. Hebbard, Nucl. Phys. **19**, 511 (1960).

[19] S. Hinds and R. Middleton, Proc. Phys. Soc. (London) **74**, 775 (1959).

[20] B. Povh and D. F. Hebbard, Phys. Rev. **115**, 608 (1959).

[21] G. M. Bailey and D. F. Hebbard, Nucl. Phys. **46**, 529 (1963).

[22] D. F. Hebbard aud G. M. Bailey, Nucl. Phys. **49**, 666 (1963).

assignment of $J^\pi \leqslant \frac{5}{2}^-$ is made[23] for the 6.16-MeV level and one of the two levels at 6.79 and 6.85 MeV appears[24,25] to be formed by $l_p=0$ and so has $J^\pi=\frac{1}{2}^+$ or $\frac{3}{2}^+$. However, there exists only a suggestion[20] that the level in question is the one at an excitation of 6.79 MeV. There appears to be no conclusive information on the spin-parity assignments of the O^{15} 6.85- and 7.17-MeV levels.[1,2,25]

The spin-parity assignments shown in Fig. 1 for the unbound levels of O^{15} follow Lauritsen and Ajzenberg-Selove[2] except for the 8.92- and 8.98-MeV levels, which follow the $N^{14}(p,\gamma)O^{15}$ work of Evans and Marion[26] and the $N^{14}(p,p)N^{14}$ work of Hagedorn *et al.*[27]

The reactions used to populate the N^{15} and O^{15} levels in the present study were $C^{13}(He^3,p)N^{15}$ ($Q=10.666$ MeV), $C^{13}(He^3,n)O^{15}$ ($Q=7.123$ MeV), $C^{14}(d,n)N^{15}$ ($Q=7.983$ MeV), $N^{14}(d,p)N^{15}$ ($Q=8.610$ MeV), $N^{14}(d,n)O^{15}$ ($Q=5.066$ MeV), and $O^{16}(He^3,\alpha)O^{15}$ ($Q=4.908$ MeV). Bombarding energies between 1.9 and 3.4 MeV for deuterons and up to 6.7 MeV for doubly ionized He^3 ions were used so that it was energetically possible to populate all the bound levels of N^{15} and O^{15} with these reactions.

The measurements which we have made can be divided roughly into three groups. Firstly, gamma-ray branching ratios were obtained from particle-gamma and gamma-gamma coincidence measurements and from three-crystal pair and Li-Ge spectra. Secondly, some information was obtained from gamma-ray angular distribution measurements performed with three-crystal pair spectrometer. Thirdly, the multipolarities of some ground-state transitions were determined from studies of the positron-electron internal pairs.

In Sec. II is described a survey of gamma rays emitted in the reactions listed above performed with the three-crystal pair spectrometer for gamma rays with energies greater than about 2 MeV. In Sec. III the particle-gamma and gamma-gamma coincidence studies are described and Sec. IV contains a description of measurements and results obtained with a Li-Ge detector. The results obtained in the study of the internal pairs are given in Sec. V. Finally, these different measurements—which are quite interdependent—are synthesized in Sec. VI.

II. THREE-CRYSTAL PAIR SPECTROMETER MEASUREMENTS

A. Procedures

The design of the three-crystal pair spectrometer, as well as its operation and the methods used in analyzing the data, have been described in detail previously.[28,29] Briefly, the three NaI(Tl) detectors of the spectrometer are fixed within a lead casting mounted on a platform whose axis of rotation has been carefully adjusted to coincide with the target center. The spectrometer is placed with a distance of ~4 in. between the front face of the central detector [a 1.5×3-in. NaI(Tl) crystal] and the target, while the gamma flux is limited to the central region of this detector by a lead collimator with a 1-in. bore. Amplified pulses from the center detector were analyzed by a 400-channel RIDL analyzer gated by an external triple coincidence circuit.

The targets used in the measurements described separately below were located at the center of a cylindrical chamber, and were placed at an angle of 45° with respect to the incident particle beam so as to minimize absorption effects within the range of angles studied ($0° \leqslant \theta_\gamma \leqslant 90°$). A standard current integrator recorded the net charge deposited during each bombardment, while a 3×3-in. NaI(Tl) detector was used to monitor the reaction gamma flux. Through the procedures outlined previously for aligning the angular distribution apparatus and stabilizing the detector circuitry possible errors in the measured angular distributions due to these sources were held to an estimated maximum of 2%.

B. Results

The $N^{14}(d,p\gamma)N^{15}$ and $N^{14}(d,n\gamma)O^{15}$ Reactions

The pair spectrum measured at a deuteron bombarding energy of 3.0 MeV and a detection angle $\theta_\gamma=55°$ is shown in Fig. 2. These data were obtained with a run of approximately 80 min at a beam current of 0.04 μA and a detector-target distance in this case of 8-in. The N^{14} target was prepared by puddling a mixture of columbium nitride and water on a 10 mil tantalum backing and then evaporating the water to make a thick (~500 keV) target that held up well under prolonged bombardment.

The solid curve through the data points of Fig. 2 shows the fitted spectrum obtained through a computer analysis (described previously[28]) which was used to determine peak areas and subsequently line intensities. With the exception of the 3.09-MeV transition from the $C^{12}(d,p\gamma)C^{13}$ reaction and the 4.43-MeV transition from the $N^{14}(d,\alpha\gamma)C^{12}$ reaction, the prominent peaks are assigned to transitions in N^{15} and O^{15} on the basis of their energies and from the results presented in Secs. III, IV, and V. Only those peaks assumed present in performing the computer analyses are indicated in

[23] W. H. Evans, T. S. Green, and R. Middleton, Proc. Phys. Soc. (London) **A66**, 108 (1953).

[24] A. J. Elwyn, J. V. Kane, S. Ofer, and R. Pixley, Phys. Rev. **120**, 2207 (1960).

[25] W. W. Rolland, Ph.D. thesis, Duke University, 1963 (unpublished).

[26] A. E. Evans and J. B. Marion, Bull. Am. Phys. Soc. **10**, 37 (1965); A. E. Evans, Ph.D. thesis, University of Maryland, 1965 (unpublished).

[27] F. B. Hagedorn, F. S. Mozer, T. S. Webb, W. A. Fowler, and C. C. Lauritsen, Phys. Rev. **105**, 219 (1957).

[28] E. K. Warburton, J. W. Olness, D. E. Alburger, D. J. Bredin, and L. F. Chase, Jr., Phys. Rev. **134**, B338 (1964).

[29] J. W. Olness, E. K. Warburton, D. E. Alburger, and J. A. Becker, Phys. Rev. **139**, B512 (1965).

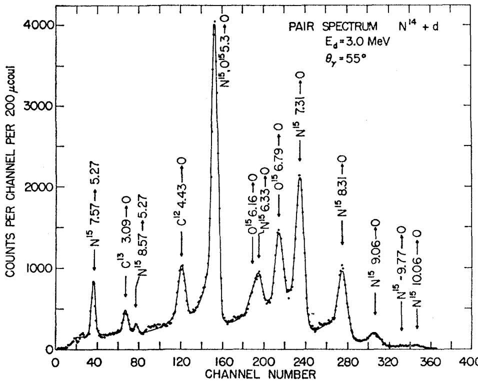

FIG. 2. Gamma-ray pulse-height spectrum measured with a three-crystal pair spectrometer following bombardment of a N^{14} target with 3.0-MeV deuterons. Transitions are identified by the nucleus and the energies (in MeV) of the initial and final levels between which the transition occur. Carbon contamination gives rise to the C^{13} 3.09 → 0 transition through the $C^{12}(d,p)C^{13}$ reaction. The other transitions identified arise from $N^{14}+d$ reactions. These data were obtained at an angle $\theta_\gamma=55°$ as part of the angular-distribution measurements described in the text. The solid curve through the experimental points is the result of a computer fit to the data which was employed to determine gamma-ray intensities.

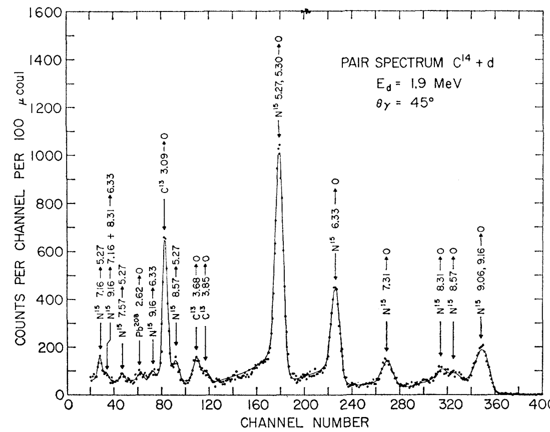

FIG. 3. Gamma-ray pulse-height spectrum measured with a three-crystal pair spectrometer following bombardment of a C^{14} target with 1.9-MeV deuterons. The transitions identified all arise from $C^{14}+d$ or $C^{12}+d$ except the 2.62-MeV peak which arises primarily from inelastic scattering of neutrons in the lead shielding of the pair spectrometer. The solid curve through the experimental points is the result of a computer fit employed to determine gamma-ray intensities.

Fig. 2, and they are labeled according to the energies of the initial and final levels of the nucleus between which the transition occurs. Although the presence of the 3.68- and 3.85-MeV gamma rays from the $C^{13}(d,p\gamma)$-C^{13} reaction is discernible, this particular region of data was excluded from the over-all fitting procedure by assigning weights of zero to the appropriate datum points.

Similar measurements and analyses were carried out for five detection angles $0°\leqslant\theta_\gamma\leqslant 90°$. The angular dependence of the line intensities thus determined were fitted with the functional form $W(\theta)=I_\gamma \sum_\nu a_\nu P_\nu(\cos\theta)$, with $a_0=1$, for even values of ν for $\nu_{\max}\leqslant 4$. The results

TABLE I. Relative intensities and angular distribution coefficients from three-crystal pair-spectrometer measurements of $N^{14}+d$ at $E_d=3.0$ MeV.

E_γ (MeV)	Assignment	I_γ (arb. units)	a_2 (%)	a_4 (%)
10.06[a]	N^{15} 10.06 → 0	4.1±0.2	−23±9	0±9
9.8	N^{15} 9.77 → 0	1.0±0.3	36±44	15±50
9.06[b]	N^{15} 9.06 → 0	14.5±0.3	1±3	1±4
8.57	N^{15} 8.57 → 0	2.2±0.4[d]	...	...
8.31	N^{15} 8.31 → 0	61.4±0.6	1±2	−1±2
7.57	N^{15} 7.57 → 0	<1[d]	...	...
7.31	N^{15} 7.31 → 0	112.4±1.0	−4.7±1.6	0.5±2
7.16	N^{15}, O^{15} 7.16 → 0	<5[d]	...	...
6.85	O^{15} 6.85 → 0	<5[d]	...	...
6.79	O^{15} 6.79 → 0	53±1	−6±3	3±3
6.33	N^{15} 6.33 → 0	24.5±1.3	−14±9	3±12
6.16	O^{15} 6.16 → 0	7.3±1.2	7±30	20±40
5.3[c]	N^{15}, O^{15} 5.3 → 0	164.1±1.2	9±2	−1±2
4.43	C^{12} 4.43 → 0	31.1±0.7	4.1±4.3	−0.3±5
3.29	N^{15} 8.57 → 5.27	4.0±0.4	6.3±18	8±21
2.83	N^{15} 9.16 → 6.33	~1.5	...	...
2.73	N^{15} 9.06 → 6.33	<0.5	...	...
2.30	N^{15} 7.57 → 5.27	44.7±1.1	−4.5±4.8	−5.6±5

[a] Contains ~16% contribution from the N^{15} 9.94 → 0 transition.
[b] Contains a (22±5)% contribution from the N^{15} 9.16 → 0 transition.
[c] Unresolved quadruplet due to the ground-state decays of the N^{15} 5.27- and 5.30-MeV levels and the O^{15} 5.19- and 5.24-MeV levels.
[d] Determined with the magnetic spectrometer and/or the Li-Ge detector.

of our measurements for $N^{14}+d$ are summarized in Table I, which lists for each transition studied the gamma-ray energy (nominal), the nuclear levels between which the transition takes place, and the solutions for the angular distribution coefficients a_2 and a_4. The relative intensities given in Table I were determined from the fitted angular distributions and peak areas using the pair-efficiency curves given previously.[28] A peak of ~2.83 MeV (not fitted in Fig. 2) corresponding to the N^{15} 9.16 → 6.33 transition was apparent in the angular distribution data and an estimate of its intensity is provided in Table I. Similarly, from the absence of a peak at 2.73 MeV, an upper limit has been set for the intensity of a possible N^{15} 9.06→6.33 transition. Additional measurements (to be discussed in following sections) utilizing the finer resolution of the magnetic spectrometer and also a Li-Ge detector have also been incorporated here to determine the relative intensities of possible ground-state transitions which were relatively too weak to have been evident in the three-crystal pair data. These additions are so labeled in Table I. The uncertainties listed in Table I are statistical and do not include possible systematic errors of ~5%.

The $C^{14}(d,n\gamma)N^{15}$ Reaction

The analysis of the data and presentation of results is completely analogous to that of the preceding reaction just described. Figure 3 shows the pair spectrum measured at $E_d=1.9$ MeV and $\theta_\gamma=45°$. Data were recorded with $E_d=1.9$ MeV at five angles of observation at a bombarding current in this case of ~0.1 μA; a spectrum was also taken at $\theta_\gamma=55°$ and $E_d=3.4$ MeV. The target was obtained through the courtesy of J. N.

TABLE II. Relative intensities and angular distribution coefficients from three-crystal pair-spectrometer measurements of $C^{14}+d$ at $E_d=1.9$ MeV.

E_γ (MeV)	Assignment	I_γ (arb. units)	a_2 (%)	a_4 (%)
9.16	N^{15} 9.16 → 0	23±6[a]		
9.06	N^{15} 9.06 → 0	47±6[a]	3.7±1.5	−1.5±1.8
8.57	N^{15} 8.57 → 0	12±3	−2.1±2.8	−0.4±3.2
8.31	N^{15} 8.31 → 0	17±3		
7.31	N^{15} 7.31 → 0	36±3	−3.1±3.4	−4.1±3.9
6.33	N^{15} 6.33 → 0	95±3	24.5±1.6	−2.1±1.8
5.30	N^{15} 5.30 → 0	210±11	2.0±1.1	−2.0±1.1
5.27	N^{15} 5.27 → 0			
3.30	N^{15} 8.57 → 5.27	19±2		
2.83	N^{15} 9.16 → 6.33	7±2		
2.73	N^{15} 9.06 → 6.33	<2		
2.30	N^{15} 7.57 → 5.27	9±3		
1.98	N^{15} 9.16 → 7.16 +8.31 → 6.33	16±6		
1.89	N^{15} 7.16 → 5.27 +9.16 → 7.31	52±6		

[a] The intensity of the 9.16–9.06 doublet was measured to be 70±4. The relative intensities of the two lines were determined with the magnetic spectrometer.

McGruer[30] and was formed by electro-deposition of acetylene gas, enriched to ~80% in C^{14}, on a 0.7 mg/cm^2 gold backing. An additional backing of 10 mil Ta was used to stop the deuteron beam. The solid curve through the data points of Fig. 3 show the results of the computer fit which was used to determine transition intensities. In this case the angular distribution data were analyzed by summing over peak regions and subtracting off appropriate tails, treating the 9.06–9.16 doublet and also the 8.31–8.57 "doublet" as single peaks. The results for $E_d=1.9$ MeV are summarized in Table II, which lists transition energies, assignments, relative intensities, and the angular distribution coefficients a_2 and a_4. Additional measurements with the Li–Ge detector disclose that the 1.89-MeV peak is due primarily to the N^{15} 7.16 → 5.27 transition, although a small contribution from N^{15} 9.16 → 7.31 is indeed present. Again, from the absence of a peak at 2.76 MeV an upper limit is set for the intensity of a possible N^{15} 9.06 → 6.33 transition. The determination of the relative contributions of the 9.06 → 0 and 9.16 → 0 transitions to the unresolved doublet intensity of 70±4 was obtained from the results of additional measurements with the magnetic pair spectrometer. The 2.62-MeV transition arises from the $Pb^{208}(n,n'\gamma)Pb^{208}$ reaction in the lead shielding of the detector. The presence of a negative a_4 term for all the angular distributions of Table II suggests a small misalignment of the apparatus since most of the initial states have $J\leqslant\frac{3}{2}$. Thus an angular distribution different from isotropy is definitely indicated for only the N^{15} 6.33 → 0 transition.

[30] The C^{14} and C^{13} targets used in this work were supplied by J. N. McGruer of the University of Pittsburgh and L. F. Chase, Jr., of the Lockheed Missiles and Space Research Laboratory, respectively.

The $O^{16}(He^3,\alpha\gamma)O^{15}$ Reaction

The pair spectrum shown in Fig. 4 exhibits the doublet peak at 5.2 MeV from the $O^{16}(He^3,\alpha\gamma)O^{15}$ reaction, while the remainder of the prominent lines presumably arise from levels in F^{18} populated by the $O^{16}(He^3,p)F^{18*}$ reaction. These data were recorded at a He^3 bombarding energy of 3.2 MeV using a beam current of 0.8 μA and a 1-mm thick target of quartz (SiO_2). The solid curve drawn through the data points represents in this case merely a hand-smoothing of statistical fluctuations. The assignment of the lower energy peaks as due to transitions in F^{18} is based on the determination of their energies and on the decay schemes for the lower lying levels of F^{18} as established by Poletti and Warburton[31] through proton-gamma coincidence measurements on the $O^{16}(He^3,p\gamma)F^{18}$ reaction. The 1.53-MeV peak presumably arises from accidentals involving annihilation radiation. Although the origins of the 1.87-, 2.70-, 3.57-, and 3.8-MeV peaks are not certain, they most probably arise from transitions involving somewhat higher lying levels of F^{18} whose decay schemes are not quite so well known. The results of the angular distribution measurements are summarized in Table III, which lists in order the transition energy, the energies of the initial and final levels of the nucleus between which the transition occurs, and the solutions for the coefficients a_2 and a_4.

The nonzero coefficient of $P_4(\cos\theta)$ in the 5.3-MeV doublet angular distribution demands that one of these two levels of O^{15} has $J\geqslant\frac{5}{2}$. Since the 5.19-MeV

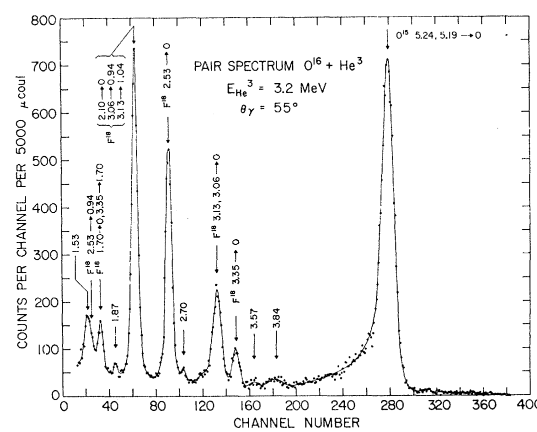

FIGURE

FIG. 4. Gamma-ray pulse-height spectrum measured with a three-crystal pair spectrometer following bombardment of a thick quartz (SiO_2) target with a 3.2-MeV He^3 beam. The transitions identified as arising from the $O^{16}(He^3,p\gamma)F^{18}$ and $O^{16}(He^3,\alpha\gamma)$-$O^{15}$ reactions are labeled by the final nucleus and the energies (in MeV) of the initial and final levels between which the transitions occur. The origin of the five peaks marked by their energies (in MeV) alone is not certain. These data were obtained at $\theta_\gamma=55°$ as part of the angular-distribution measurements described in the text. The solid curve through the experimental points is a hand-smoothing of the experimental data.

[31] A. R. Poletti and E. K. Warburton, Phys. Rev. **137**, B595 (1965).

TABLE III. Angular distribution coefficients from three-crystal pair-spectrometer measurements of $O^{16}+He^3$ at $E_{He^3}=3.2$ MeV.

E_γ (MeV)	Assignment	a_2 (%)	a_4 (%)
5.3	O^{15} 5.24 → 0 + 5.19 → 0	24±2	−32±2
3.84	F^{18} (?)	64±10	31±12
3.35	F^{18} 3.35 → 0	43±9	−3±9
3.1	F^{18} 3.13 → 0 + 3.06 → 0	6±4	0±4
2.53	F^{18} 2.53 → 0	−19±3	42±3
2.1	F^{18} 3.13 → 1.04 + 3.06 → 0.94 + 2.10 → 0	−24±3	−3±2

level has $J=\frac{1}{2}^+$, it is the 5.24-MeV level which has $J\geq\frac{5}{2}$. The limit $J\geq\frac{5}{2}$ for the O^{15} 5.24-MeV level agrees with the recent determination[7] of $J=\frac{5}{2}$ for this level.

With respect to the levels of F^{18}, the observation of a large $P_4(\cos\theta)$ term in the 2.53-MeV gamma-ray angular distribution is in agreement with the results of Poletti and Warburton,[31] who observed a large P_4 term in the p-γ correlation and concluded the level has $J=2$ and decays with an appreciable quadrupole component. Our results for the other F^{18} transitions are also consistent with the conclusions of Poletti and Warburton.

The $C^{13}(He^3,p\gamma)N^{15}$ and $C^{13}(He^3,n\gamma)O^{15}$ Reactions

Figure 5 shows the three-crystal pair spectrum measured at a bombarding energy of 2.9 MeV and a detection angle of 45°. The target for these measurements was obtained from L. F. Chase, Jr.,[30] and consisted of a ~25 μg/cm² thick layer of carbon (33% C^{12}–67% C^{13}) on a thin gold backing. A bombarding energy of 2.9 MeV was selected since this is below the energy for resonance formation of the 6.44-MeV level of N^{14} through the $C^{12}(He^3,p\gamma)N^{14}$ reaction. Previous measurements[28] at this energy with a C^{12} target have determined the spectral shape due to the latter reaction, and hence its contribution to the spectrum of Fig. 5 is readily accounted for. The identification of various transitions in N^{14} is based on these previous results, and the transitions are labeled according to the energies of the initial and final levels of N^{14} between which these transitions occur. The solid curve is the result of a computer fit to the data. In addition to the various ground-state transitions evident in Fig. 5, there is also a strong 4.56-MeV peak due to the 9.83 → 5.27 transition in N^{15}. This peak contains a small contribution from the C^{12} 4.43-MeV gamma ray. Also, the intensity of the 3.9-MeV peak is too strong to be ascribed entirely to the N^{14} 6.21 → 2.31 transition from $C^{12}(He^3,p\gamma)N^{14}$ (see Fig. 1 of Ref. 8) indicating the presence of a second component subsequently found (see Sec. IV) to arise from the 9.23 → 5.30 transition in N^{15}. The high-energy region is shown in expanded scale in the inset of Fig. 5. The peak energies determined by the fitting procedure are designated in this insert by the arrows above the curve. From the evident correspondences between the expected and generated peak positions, we conclude that the most intense ground-state transitions in the $C^{13}(He^3,p)N^{15}$ reaction are those from the 9.16-, 9.77-, 10.06-, and 10.81-MeV levels and that the 9.06-, 9.94-, and 10.45-MeV levels give relatively weaker ground-state transitions. We know from other evidence (Sec. III) that the 9.83-MeV level of N^{15} has a small ground-state branch or none at all. Of interest here is weak evidence for an additional gamma ray of 9.27±0.06 MeV. This gamma ray, if present, would presumably correspond to a ground-state transition from the 9.23-MeV level of N^{15}.

The results of these measurements are summarized in the first 3 columns of Table IV, which list, respectively, the gamma-ray energy (nominal), its assignment to the N^{15} or O^{15} level scheme, and its relative intensity. The results of previous measurements with a C^{12} target are shown for comparison in columns 4 and 5, where the intensities have been normalized to correspond to the present measurements.

III. GAMMA-RAY COINCIDENCE STUDIES

A. Proton-Gamma Coincidence Measurements

The gamma-ray decay modes of the bound levels of N^{15} were investigated by two-parameter analysis of proton-gamma coincidence spectra from the $C^{13}(He^3,p\gamma)N^{15}$ and $N^{14}(d,p\gamma)N^{15}$ reactions.

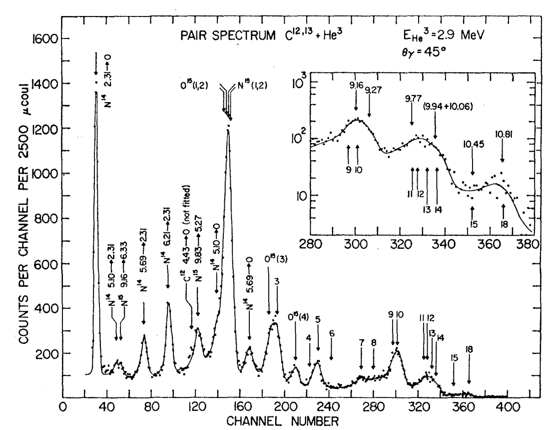

FIG. 5. Gamma-ray pulse-height spectrum measured with a three-crystal pair spectrometer following bombardment of a $C^{12,13}$ target with a 2.9-MeV He^3 beam. The transitions from $C^{12}(He^3,p\gamma)N^{14}$, $C^{13}(He^3,\alpha\gamma)C^{12}$, and the cascade transitions from $C^{13}(He^3,p\gamma)N^{15}$ are labeled by the final nucleus and the energies (in MeV) of the initial and final levels between which the transitions occur. Ground-state transitions in N^{15} are labeled by the level sequence, in order of increasing excitation energy, of Fig. 1 (excluding the 9.23-MeV level). Ground-state transitions in O^{15} are labeled by O^{15} followed by the level sequence (in parenthesis). These data were obtained at $\theta_\gamma=45°$. The solid curve through the experimental points is a computer fit employed to determine gamma-ray intensities. The insert shows the high-energy region in more detail. The arrows below the experimental curve in this insert give the expected positions of the ground-state transitions The arrows above the experimental curve give the positions generated by the computer fit for the six peaks assumed in the analysis.

TABLE IV. Gamma-ray intensities from three-crystal pair-spectrometer measurements on $C^{12,13}+He^3$ at $E_{He^3}=2.9$ MeV. Similar results for $C^{12}+He^3$ are shown for comparison.

	$C^{12,13}+He^3$ (present work)		$C^{12}+He^3$ (Ref. 28)	
E_γ (MeV)	Assignment	I_γ (arb. units)	E_γ (MeV)	I_γ[a]
10.81	N^{15} 10.81 → 0	8.2±1		
10.45	N^{15} 10.45 → 0	2.6±3		
10.00	N^{15} 10.06 → 0	29±4		
	+9.94 → 0			
9.77	N^{15} 9.77 → 0	22±4		
9.27	(N^{15} 9.23 → 0)	≲10		
9.16	N^{15} 9.16 → 0	65±16		
	+9.06 → 0			
8.57	N^{15} 8.57 → 0	2.7±1.4		
8.31	N^{15} 8.31 → 0	11±3		
7.31	N^{15} 7.31 → 0	35±4		
6.79	O^{15} 6.79 → 0	22±3		
6.33	N^{15} 6.33 → 0	65±7	6.44	14±1
6.16	O^{15} 6.16 → 0	50±7	6.21	15±1
			5.83	7±2
5.69	N^{14} 5.69 → 0	36±3	5.69	33±2
5.30	N^{15}, O^{15} (5.3) → 0	340±2		
5.10	N^{14} 5.10 → 0	(34±5)	5.10	62±4
			4.91	20±4
4.56	N^{15} 9.83 → 5.27	38±3		
3.90	N^{14} 6.21 → 2.31	75±4	3.90	56±3
	+N^{15} 9.23 → 5.3			
3.38	N^{14} 5.69 → 2.31	47±4	3.38	48±3
	N^{15} 9.16 → 6.33	13±4		
2.85	+N^{15} 9.22 → 6.33			
2.79	N^{14} 5.10 → 2.31	16±5	2.79	22±3
2.31	N^{14} 2.31 → 0	460±30	2.31	452±20

[a] Normalized to the N^{14} peak intensities for $C^{12,13}+He^3$.

The C^{13} target consisted of a self-supporting foil of carbon containing about 60% C^{13} prepared by cracking methyl iodide. This target was about 40-keV thick for 3-MeV He^3 ions.[30] The N^{14} target was prepared by vacuum evaporation of adenine ($C_5H_3N_4 \cdot NH_2$) onto a 30 μg/cm² film of VYNS.[32] This target contained about 200 μg/cm² of adenine and was ~40-keV thick for 3-MeV deuterons.

The proton-gamma coincidence measurements were carried out with the targets located at the center of a cylindrical scattering chamber with an angle of 45° between the target normal and the incident beam direction. The charged-particle beam from the Van de Graaff accelerator was limited to a diameter of 1 mm by a tantalum collimator located at the chamber entrance. Charged reaction products were detected using a silicon surface barrier counter at 70° to the incident beam direction at a distance of 1.5 cm from the target. The angular spread of the reaction products was limited to $\Delta\theta \sim 10°$ by a set of tantalum slits at the detector face. The gamma-ray detector was a 5×5-in. NaI(Tl) crystal placed directly above the target and at a distance of 2 cm from the target. The cover-plate of the scattering chamber was made from lucite and cut out to a thickness of $\frac{1}{4}$ in. between the target and gamma-ray detector in order to minimize absorption effects. Amplified coincidence pulses from the gamma detector and the proton detector were analyzed by a TMC 16 384-channel, two-parameter analyzer used in its 128×128-channel mode. The necessary coincidence conditions were imposed by an external coincidence circuit ($\tau=100$ nsec) which gated the two-parameter analyzer.

[32] B. D. Pate and Y. Yaffe, Can. J. Chem. 33, 15 (1954).

Both reactions were investigated at a bombarding energy of 3.0 MeV. A 24-h run was performed on the $C^{13}(He^3,p\gamma)N^{15}$ reaction with a He^3 current of ~0.1 μA. The proton-gamma coincidence spectrum from the $N^{14}(d,p\gamma)N^{15}$ reaction was measured with a beam current of ~0.003 μA and a duration of 20 h.

The results were initially displayed by plotting the charged-particle spectra in coincidence with various gamma-ray energy increments. Five such plots are shown in Fig. 6 for $C^{12,13}+He^3$. The spectra of Fig. 6 were generated by a computer program which printed out the spectra along one axis of the two-dimensional analyzer in coincidence with any chosen group of channels along the other axis. An option of this program allowed the subtraction of one or two such spectra, normalized to the number of added channels from a third. This option was used in background subtraction and in separating the contributions of unresolved peaks.

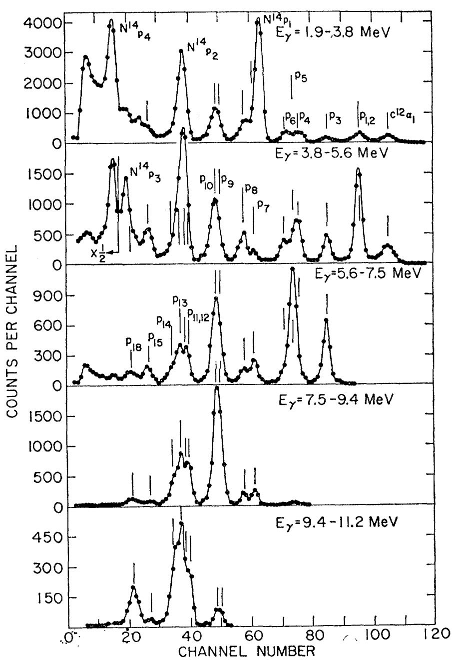

FIG. 6. Charged-particle spectra at 70° to the beam from $C^{12,13}+He^3$ at $E_{He^3}=3.0$ MeV. The spectra were generated from a two-dimensional particle-gamma coincidence spectra by displaying the charged-particle spectra in coincidence with the indicated gamma-ray energy increments. The peaks arising from $C^{13}(He^3,\alpha\gamma)C^{12}$ ($Q=15.630$ MeV) and $C^{12}(He^3,p\gamma)N^{14}$ ($Q=4.779$ MeV) are identified by the final nucleus and the sequence of the levels. The proton peaks from $C^{13}(He^3,p\gamma)N^{15}$ are identified by the level sequence only. The sequence is that of Fig. 1 with the 9.23-MeV level omitted. Proton groups from $O^{16}(He^3,p\gamma)F^{18}$ ($Q=2.021$ MeV) were also seen in coincidence with gamma rays with energies less than 1.9 MeV.

Another option simulated the 128×128 matrix of accidental counts from proton and gamma-ray singles spectra, normalized this matrix to a given random/real ratio, and subtracted it from the measured 128×128 matrix of counts.

The random/real coincidence ratio for both measurements was about 1/10. However, most of the random counts occurred in the region of gamma-ray energy below 1 MeV and in the gamma-ray energy region of interest the random/real ratio was considerably less than $\frac{1}{10}$ and the subtraction of the random-coincidence spectra was performed with negligible error. All the gamma-ray spectra which will be shown have been thus corrected.

We shall consider the results obtained from the $C^{13}(He^3,p\gamma)N^{15}$ reaction first. The gamma-ray spectrum from the decay of the unresolved 5.27-, 5.30-MeV doublet ($p_{1,2}$) of N^{15} is shown in Fig. 7(a). This plot shows the gamma-spectrum obtained in coincidence with six proton channels summed over the $p_{1,2}$ group (Fig. 6). Figure 7(b) shows the gamma-ray spectrum from the decay of the 6.33-MeV level of N^{15} which was obtained by summing the data over five channels corresponding to the proton group p_3. These two spectra obtained from the $C^{13}(He^3,p\gamma)N^{15}$ reaction give the response of the NaI(Tl) detector to 5.3- and 6.3-MeV gamma rays and were useful in decomposing more complex spectra.

Two complex spectra from unresolved peaks are shown in Figs. 8(a) and 8(b). Figure 8(a) shows the gamma-ray spectrum in coincidence with five channels centered on the proton groups p_4, p_5, p_6; while Fig. 8(b) shows the spectrum coincident with proton groups p_{11-14}.

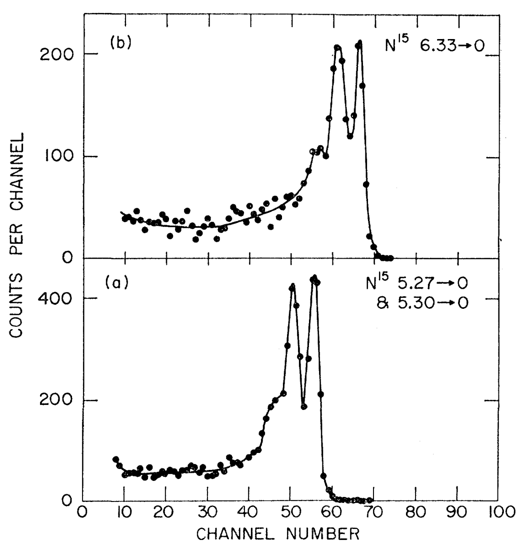

FIG. 7. Gamma-ray spectra from $C^{13}(He^3,p\gamma)N^{15}$ at $\theta_\gamma=90°$ and $E_{He^3}=3.0$ MeV in coincidence with the proton groups feeding (a) the N^{15} 5.270-, 5.299-MeV doublet and (b) the N^{15} 6.33-MeV level.

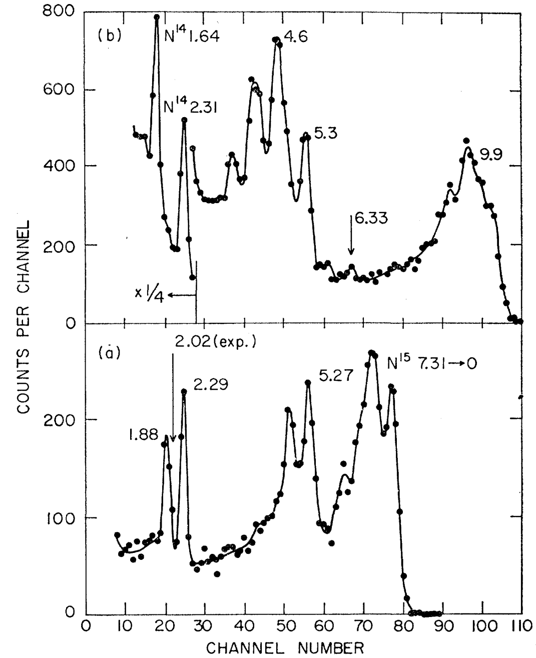

FIG. 8. Gamma-ray spectra from $C^{12,13}+He^3$ at $\theta_\gamma=90°$ and $E_{He^3}=3.0$ MeV in coincidence with the proton groups feeding (a) the N^{15} 7.16-, 7.31-, and 7.57-MeV triplet and (b) the N^{15} 9.77-, 9.83-, 9.94-, and 10.06-MeV quadruplet and the N^{14} 3.95-MeV level. Gamma-ray peak energies are given in MeV.

The spectrum of Fig. 8(a) is consistent with the reported decay modes of the N^{15} 7.16-, 7.31-, and 7.57-MeV levels and with the results presented in Table I. The 7.16- and 7.57-MeV levels decay by cascade through the 5.27-MeV level, with ground-state branches of less than 5%[8]; while the 7.31-MeV level decays predominantly to the ground state with no reported cascades.[3]

From present results we can set limits on cascades from all three of these levels through the N^{15} 6.33-MeV level and on cascades from the 7.31-MeV level through the 5.3-MeV doublet. This is done by enhancing the relative contribution of the decay of one of these levels by summing a smaller number of proton channels and subtracting the spectrum in coincidence with adjacent channels. However, no useful information can be obtained from these results on the ground-state branches from the 7.16- and 7.57-MeV levels since the gamma-ray detection efficiency in this work was about 20% for gamma rays with minimum absorption. Thus, the summing correction for cascades is also about 20% and a ground-state branch of 5% would therefore not be discernible.

The spectrum of Fig. 8(b) shows intense gamma rays of 1.64 and 2.31 MeV from the $C^{12}(He^3,p)N^{14}$ reaction populating the N^{14} 3.95-MeV level which decays[1] 96% of the time by cascade through the 2.31-MeV first-excited state of N^{14}. The other gamma-ray peaks in Fig. 8(b) are due to the decay of the four N^{15} levels corresponding to p_{11-14} (Fig. 6). It is impossible to completely separate the gamma-ray spectra due to these four levels; in the present measurement however, it is evident from Fig. 6 that the levels contributing to the unresolved quartet p_{11-14} have dissimilar decay modes and that both p_{14} and p_{13} and either one or both of p_{12} and p_{11} are contributing to this quartet. Additional information contained in the 128×128 two-dimensional matrix can be displayed by plotting, as a function of proton channel, the ratio of counts in the regions $E_\gamma=9.4$–11.2 MeV and 3.8–5.6 MeV. When this is done it is evident that all four levels are contributing to Fig. 8(b), that the 10.06-MeV level (p_{14}) decays predominantly by a ground-state transition, the 9.83-MeV level (p_{12}) decays predominantly by cascade through the 5.3-MeV doublet and the 9.77- and 9.94-MeV levels have strong ground-state branches with the possibility of appreciable cascades through the 5.3-MeV doublet. These statements were confirmed and extended by displaying computer generated gamma-ray spectra resulting from the differences between spectra in coincidence with small groups of proton channels as explained previously.

The gamma-ray spectrum associated with the proton group labeled $p_{9,10}$ in Fig. 6 was obtained by summing over seven proton channels containing the bulk of this peak and is shown in Fig. 9. The results shown in Fig. 9 seemed at first to be difficult to reconcile with other studies of the 9.06-, 9.16-MeV levels of N^{15}. For this reason a second $C^{13}(He^3,p\gamma)N^{15}$ coincidence spectrum was measured with 256 channels for the gamma-ray axis and 64 channels for the proton axis. From these data the energies of the 2.83- and 3.92-MeV

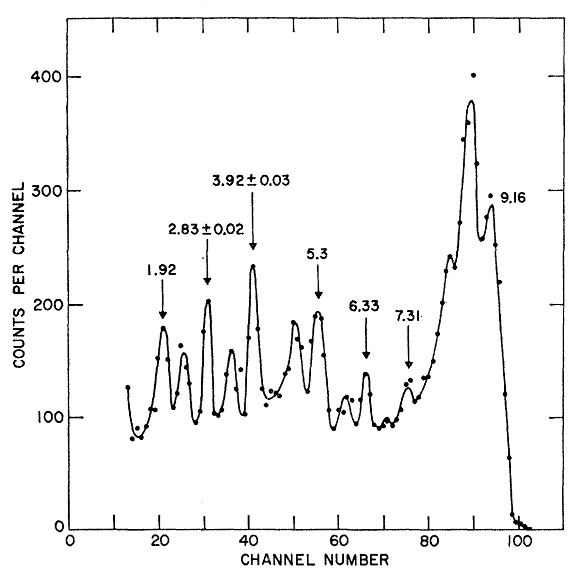

FIG. 9. Gamma-ray spectrum from $C^{13}(He^3,p\gamma)N^{15}$ at $\theta_\gamma=90°$ and $E_{He^3}=3.0$ MeV in coincidence with the proton groups feeding the 9.06-, 9.16-, and 9.23-MeV triplet. Gamma-ray peak energies are given in MeV.

peaks (shown in Fig. 9) were determined as shown and it was found also that the 1.92-MeV peak is actually a 1.89-, 2.00-MeV doublet. The gamma-gamma coincidence studies (Sec. IIIB) show that these latter two gamma rays arise from a $9.16\rightarrow7.16\rightarrow5.27$ cascade and that there is also present a weak 1.85-MeV gamma ray from a $9.16\rightarrow7.31$ cascade. The peak labeled 7.31 MeV in Fig. 9 arises from both the $9.16\rightarrow7.31\rightarrow0$ cascade and summing of two gamma rays in the $9.16\rightarrow7.16\rightarrow5.27\rightarrow0$ cascade.

The gamma-gamma coincidence measurements also show clearly that the 2.83- and 3.92-MeV gamma rays are in coincidence with the 6.33- and 5.3-MeV lines, respectively. The energies of the $9.16\rightarrow6.33$ and $9.16\rightarrow5.3$ transitions have been accurately measured[3] as 2.827 ± 0.003 and 3.854 ± 0.004 MeV, respectively. Our measurement of the energy of the 2.83-MeV gamma ray is in good agreement with the former value but it seems quite clear that the gamma ray at 3.92 ± 0.03 MeV has an energy which is too high to be associated with a $9.16\rightarrow5.3$ transition. Instead, it gives evidence for a level at 9.21 ± 0.03 MeV which we associate with the level reported at 9.231 ± 0.008 MeV[6,7] for which questionable evidence was found in the three-crystal pair spectra for $C^{13}+He^3$.

The energy calibration for the data of Fig. 6 suggests that the proton group labeled $p_{9,10}$ is due primarily to the feeding of the 9.16-MeV level. The 9.06-MeV level appears to be weakly fed, as is also indicated by the results of Fig. 5, and further, the 9.23-MeV level has a relatively weak ground-state transition.

Energy levels in N^{15} with excitation energies above 10.208 MeV can decay by proton emission to C^{14} and levels above 10.834 MeV can also decay by neutron emission to N^{14}. The proton groups labeled p_{15} and p_{18} in Fig. 6 are associated with N^{15} levels at 10.45 and 10.81 MeV. The gamma-ray spectra in coincidence with these two groups are illustrated in Figs. 10(a) and 10(b). The spectrum in Fig. 10(a) has poor statistics due to the weak intensity of p_{15} (Fig. 6) and has a background for $E_\gamma<4$ MeV from contaminant reactions including $O^{16}(He^3,p\gamma)F^{18}$. However, the major decay mode of the 10.45-MeV level is obviously by cascade through 5.3-MeV doublet with other possible decay modes indicated by the inserted decay scheme. The proton group p_{18} was only partially resolved from the N^{14} p_3 proton group feeding the 4.91-MeV level of N^{14}. However, it was possible to resolve the contributions of the 4.91-MeV gamma ray and the unresolved gamma rays from the $10.81\rightarrow5.3\rightarrow0$ cascade as indicated by the dashed curve of Fig. 10(b).

Gamma-ray emission from the N^{15} energy levels corresponding to p_{16} and p_{17} was not observed in this work. This was expected for p_{17} since the N^{15} 10.706-MeV level (p_{17}) has $\Gamma_\gamma/\Gamma\leqslant0.001$, i.e., this level decays[17] almost entirely by proton emission to C^{14}. For the N^{15} 10.543-MeV level (p_{16}), there is only the limit

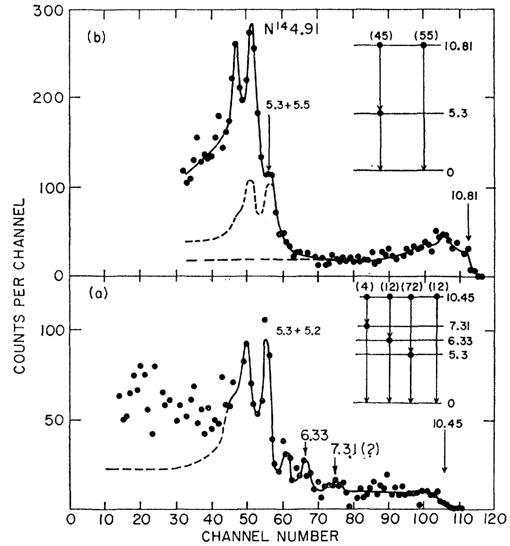

FIG. 10. Gamma-ray spectrum from $C^{12,13}+He^3$ at $\theta_\gamma=90°$ and $E_{He^3}=3.0$ MeV in coincidence with the proton groups feeding (a) the N^{15} 10.45-MeV level and (b) the N^{15} 10.81-MeV level and the N^{14} 4.91-MeV level. Gamma-ray peak energies are given in MeV. The decay schemes inferred from the spectra are indicated in the inserts.

$\Gamma_\gamma/\Gamma \leqslant 0.5$.[17] The absence of evidence for gamma rays originating from this level suggests that Γ_γ/Γ is probably considerably less than this limit. Note that the N^{15} 10.543-MeV level has a negligible ground-state branch and approximately equal cascades through the N^{15} 5.3-MeV doublet and 7.16-MeV level[17] so that the gamma-ray spectrum from the decay of this level cannot be confused with that from the decay of the 10.45-MeV level [Fig. 10(a)].

Estimates of the ratio of radiative width to total width (Γ_γ/Γ) for the N^{15} 10.45- and 10.81-MeV levels can be obtained from a comparison of the proton singles spectrum and the proton coincidence spectra.

Designating the total gamma-ray intensity observed in coincidence as $I_\gamma(10.45)$, and the proton intensity observed in the singles spectrum as $I_p(10.45)$, we can write

$$\Gamma_\gamma/\Gamma(10.45)=\{I_\gamma(10.45)/I_p(10.45)\}/\{I_\gamma(b)/I_p(b)\},$$

where the symbol b designates the corresponding quantities for some (any) bound level. We have chosen the above form to calculate $\Gamma_\gamma/\Gamma(10.45)$ and Γ_γ/Γ (10.81) utilizing the fact that $\Gamma_\gamma/\Gamma(b)\equiv 1$, since it does not require one to know the normalizing factors which must obtain between singles and coincidence spectra. The ratios indicated above were calculated for the 10.45- and 10.81-MeV levels; the bound levels referred to in this procedure were the unresolved doublets corresponding to $p_{9,10}$, $p_{7,8}$, and $p_{1,2}$. The results provide a satisfactory internal check on the procedure, yielding the values $\Gamma_\gamma/\Gamma(10.45)=1.0_{-0.15}^{+0.3}$, and $\Gamma_\gamma/\Gamma(10.81)=0.55_{-0.15}^{+0.25}$. The asymmetry in the uncertainties associated with these estimates is due to the possible presence of proton groups p_{16} and p_{17} associated with the N^{15} 10.54- and 10.71-MeV levels. These estimates of Γ_γ/Γ were obtained using the branching ratios indicated in Fig. 10.

In the studies of the $C^{13}(He^3,p)N^{15}$ reaction, the strong $C^{12}(He^3,p)N^{14}$ proton group populating the first-excited state of N^{14} at 2.31 MeV was not resolved from the N^{15} p_7 group. The presence of the intense N^{14} 2.31-MeV gamma ray obscured the region where cascade gamma rays from the 8.31- and 8.57-MeV levels were expected. Thus, the decay modes of these two levels were investigated by the $N^{14}(d,p\gamma)N^{15}$ reaction. Figures 11(a) and 11(b) illustrate the gamma-ray spectra in coincidence with p_7 and p_8 from the $N^{14}(d,p\gamma)N^{15}$ reaction. The 8.31-MeV level is strongly populated in this reaction and accurate branching ratios were determined from the decay of this level. The 8.57-MeV level was weakly populated; however, the results were in good agreement with those obtained from the $C^{13}(He^3,p\gamma)N^{15}$ reaction (from which branching ratios of 33%, 67%, and $\leqslant$7% were obtained for the $8.57\rightarrow 0$, $8.57\rightarrow 5.3$, and $8.57\rightarrow 6.33$ transitions) except for the presence in Fig. 11(b) of a gamma ray with an energy of 1.85 ± 0.1 MeV. This gamma ray was not observed in the $C^{13}(He^3,p\gamma)N^{15}$ reaction. It has the right energy to be associated with the N^{15} $7.16\rightarrow 5.27$ transition, but if there were a $8.57\rightarrow 7.16\rightarrow 5.27$ cascade then a 1.41-MeV gamma ray with an intensity equal to that of the 1.85-MeV gamma ray should be present. We conclude that the 1.85-MeV gamma ray arises from an unknown source (contaminant?) and

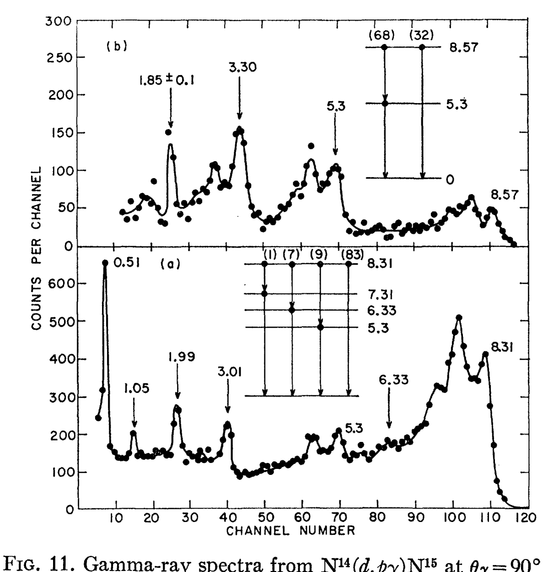

FIG. 11. Gamma-ray spectra from $N^{14}(d,p\gamma)N^{15}$ at $\theta_\gamma=90°$ and $E_d=3.0$ MeV in coincidence with the proton groups feeding (a) the 8.31-MeV level and (b) the 8.57-MeV level. The gamma-ray peak at 1.85 ± 0.1 MeV in (b) is presumed to arise from a contaminant reaction. The decay schemes inferred from the spectra are indicated in the inserts. Gamma-ray peak energies are given in MeV.

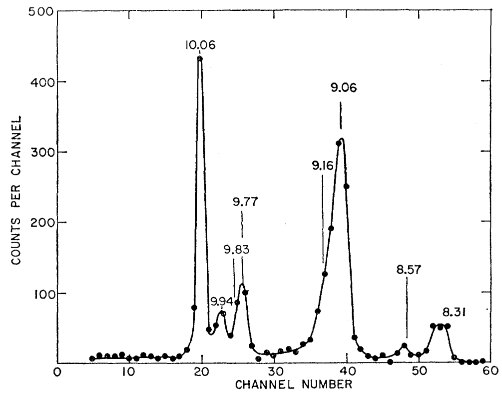

FIG. 12. Proton spectrum from $N^{14}(d,p\gamma)N^{15}$ at 70° to the beam in coincidence with gamma rays in the energy range 8.8–10.2 MeV. The proton groups are labeled by the excitation energies (in MeV) of the N^{15} levels to which they correspond.

set a limit on a possible $8.57 \rightarrow 7.16$ branch from the $C^{13}(He^3,p\gamma)N^{15}$ results and from a limit on the intensity of a possible 1.41-MeV gamma ray in Fig. 11(b).

The rest of the information obtained from the $N^{14}(d,p\gamma)N^{15}$ reaction was consistent with that obtained from the $C^{13}(He^3,p\gamma)N^{15}$ reaction. The $p_{9,10}$ doublet was not resolved from the intense C^{13} p_3 group. Some additional information was obtained on cascades from the 7.31-MeV level (p_5), in particular a $(2\pm1)\%$ branch to the 5.3-MeV doublet was observed. We present one further result from the $N^{14}(d,p\gamma)N^{15}$ reaction measurements, namely, the spectrum (Fig. 12) of protons in coincidence with gamma rays with energies in the range 8.8–10.2 MeV. This spectrum shows clearly the proton groups $p_{11,12}$, p_{13}, and p_{14} which are obscured by the C^{13} p_3 group in the proton singles spectrum and in the spectrum of protons in coincidence with all gamma rays. This spectrum confirms the existence of a N^{15} 9.94-MeV level (p_{13}) and supports the evidence for a N^{15} 9.77-MeV level (p_{11}).

No evidence was found in this work for the N^{15} levels reported[6] at excitation energies of 8.64, 8.74, and 9.60 MeV.

B. Gamma-Gamma Coincidence Measurements

Gamma-gamma coincidence measurements were performed on the de-excitation gamma rays from the bound levels of N^{15} and O^{15} using $N^{14}+d$, $C^{14}+d$, and $O^{16}+He^3$ to populate the excited states. The N^{14}, C^{14}, and O^{16} targets were the same as used in the three-crystal pair spectrometer studies (Sec. II). Measurements were made at $E_d=3.2$ MeV for $N^{14}+d$, 1.9 and 3.2 MeV for $C^{14}+d$, and 6.7 MeV for $O^{16}+He^3$.

High-energy gamma rays ($E_\gamma>4.6$ MeV) were detected by a 5×5-in. NaI(Tl) crystal at 90° to the beam and 2 cm from the target. Low-energy gamma rays ($E_\gamma<5.3$ MeV) were detected by a 3×3-in. NaI(Tl) crystal at 60° to the beam and 4 cm from the target. The coincidence measurements were performed with the TMC 16 384-channel analyzer used in its 128×128-channel mode using the same electronic conditions and methods of analysis as were used for the (p,γ) coincidence measurements. Each of the three coincidence spectra took approximately 8 h to collect.

Typical results are illustrated by Figs. 13, 14, and 15 which show some of the results from the $N^{14}+d$ measurements. Figure 13 illustrates the total coincidence spectra from both crystals, Figs. 14 and 15 illustrate the spectra coincident with various gamma-ray peaks where the contribution from the tails of higher energy gamma rays have been subtracted approximately. From spectra of this sort many previously known or suspected transitions were confirmed and limits were placed on other cascades. For instance, no transitions were observed to the N^{15} 8.57- or 8.31-MeV levels, while conclusive evidence was found for $9.16 \rightarrow 7.31$ and

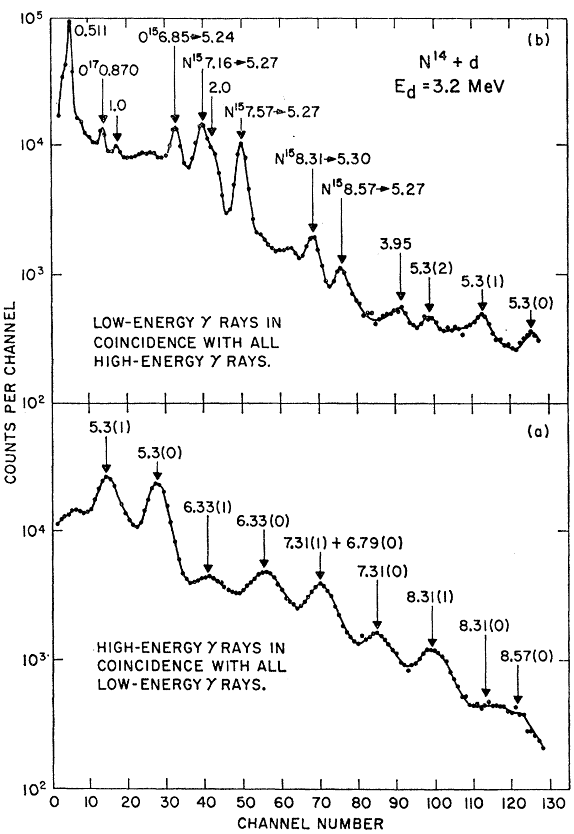

FIG. 13. Gamma-gamma coincidence spectra from $N^{14}+d$ at $E_d=3.2$ MeV. The spectra in (a) and (b) were measured in coincidence with each other. Ground-state transitions ($E_\gamma>5$ MeV) are labeled in (a) by excitation energies (in MeV) of the initial states in N^{15} or O^{15}, their full-escape peaks are labeled by (0), one-escape peaks by (1), and two-escape peaks by (2). Cascade transitions are labeled by the nucleus and the initial and final levels between which the transitions occur. The 0.511-MeV peak arises from annihilation radiation, the O^{17} 0.870-MeV peak is mostly due to accidentals and arises from the $O^{16}(d,p\gamma)O^{17}$ reaction. The origins of the 1.0-, 2.0-, and 3.95-MeV peaks are discussed in the text. In (a) the one-escape peaks are somewhat enhanced relative to full-escape peaks due to real coincidences with annihilation radiation.

$8.31 \rightarrow 7.31$ cascades. The evidence for the latter is illustrated by the spectra of Figs. 14(c) and 15(c). Quantitative branching ratios were obtained from these measurements by extracting relative intensities using crystal efficiency curves and normalizing these results to accord with the relative probabilities for feeding the various levels as determined from the three-crystal pair spectrometer results (Sec. II).

The interpretation of the gamma-gamma coincidence spectra was greatly facilitated by comparison of the results from the four different measurements since the relative populations of the various levels were quite different for the four. For instance, the relative populations of the N^{15} 8.31- and 9.16-MeV levels, as formed in the $N^{14}+d$ and $C^{14}+d$ measurements, differ by a factor of ~ 20, while for $E_d = 1.9$ MeV, states above 9.2 MeV were not populated in the $C^{14}+d$ reaction (compare Tables I and II) and for $O^{16}+He^3$ only O^{15} states were formed. The effect of these differences on

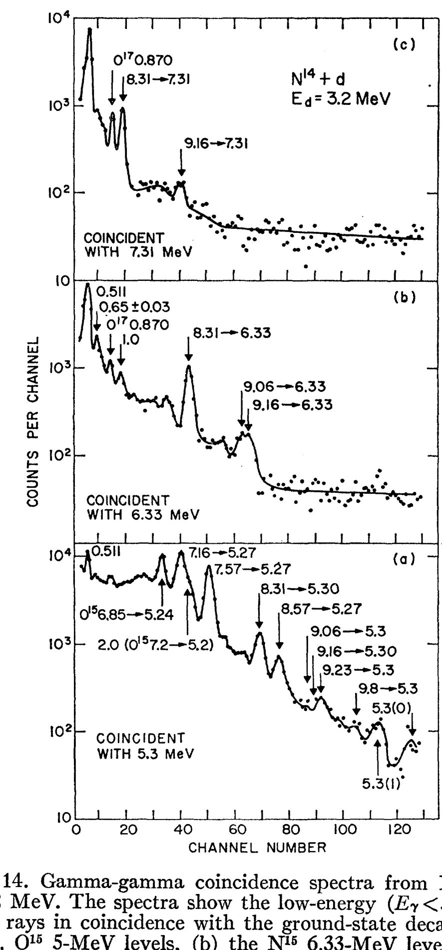

FIG. 14. Gamma-gamma coincidence spectra from $N^{14}+d$ at $E_d=3.2$ MeV. The spectra show the low-energy ($E_\gamma<5.4$ MeV) gamma rays in coincidence with the ground-state decays of (a) the N^{15}, O^{15} 5-MeV levels, (b) the N^{15} 6.33-MeV level and O^{15} 6.16-MeV level, and (c) the N^{15} 7.31-MeV level. Cascade transitions in N^{15} are labeled by the energies of the initial and final levels (in MeV) between which the transitions occur. Two O^{15} cascade transitions are also labeled in (a). The origin of the 0.511-, 0.870-, and 1.0-MeV peaks is the same as for Fig. 13. The origin of the peak at 0.65 ± 0.03 MeV is unknown.

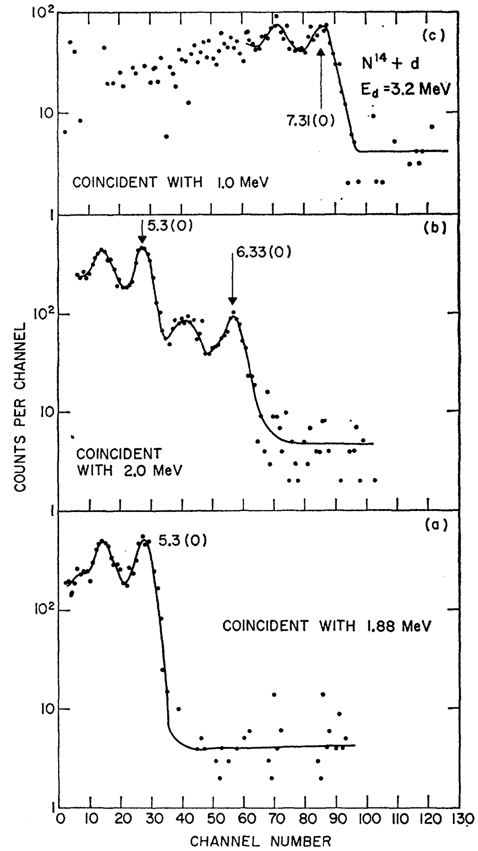

FIG. 15. Gamma-gamma coincidence spectra from $N^{14}+d$ at $E_d=3.2$ MeV. The spectra show the high-energy ($E_\gamma>4.6$ MeV) gamma rays in coincidence with (a) 1.88-MeV gamma rays, (b) 2.0-MeV gamma rays, and (c) 1.0-MeV gamma rays. The full-energy-loss peaks are labeled by their energies (in MeV).

the coincidence spectra is evident by comparing Fig. 14 with Fig. 16. For example, the spectrum of Fig. 16(c) shows conclusive evidence for a $9.16 \rightarrow 7.31$ cascade and suggests the possible presence of a $9.06 \rightarrow 7.31$ cascade. In contrast the intensity of the $9.16 \rightarrow 7.31$ cascade labeled in Fig. 14(c) could only be extracted with a large uncertainty and, in fact, the results from $N^{14}+d$ alone cannot be considered as conclusive evidence for this cascade.

The peak labeled $9.23 \rightarrow 5.3$ in Fig. 14(a) had a measured energy of 3.95 ± 0.02 MeV and thus agrees well with the expected energy of 3.953 MeV for the $9.23 \rightarrow 5.27$ transition, not so well with the energy of 3.924 expected for the $9.23 \rightarrow 5.30$ transition, and is clearly inconsistent with the energy of 3.854 MeV associated[3] with the $9.16 \rightarrow 5.30$ transition.

A rather intense 2.0-MeV gamma ray is evident in the spectrum coincidence with the 5.3-MeV lines for both $N^{14}+d$ [Fig. 14(a)] and $C^{14}+d$ [Fig. 16(a)]. In the latter case, this gamma ray is associated with the N^{15} $9.16 \rightarrow 7.16 \rightarrow 5.27 \rightarrow 0$ cascade. In the case of $N^{14}+d$ this cascade makes only a small contribution to

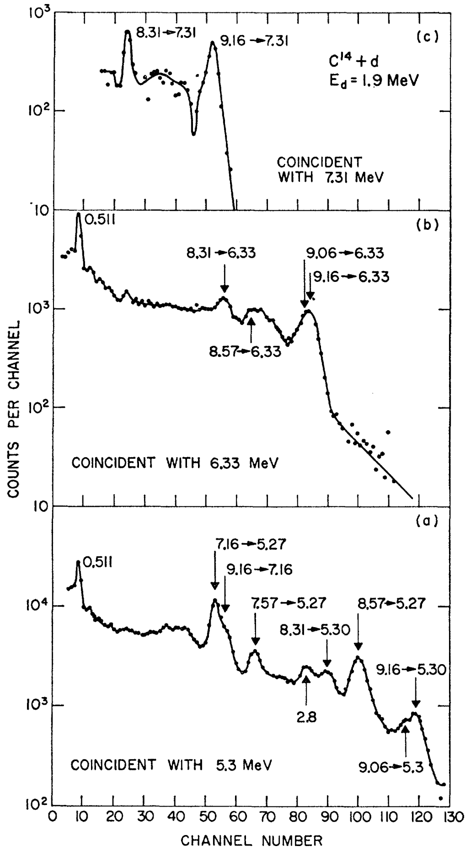

FIG. 16. Gamma-gamma coincidence spectra from $C^{14}+d$ at $E_d=1.9$ MeV. The spectra show the low-energy ($E_\gamma<4$ MeV) gamma rays in coincidence with the ground-state decays of (a) the N^{15} 5.3-MeV doublet, (b) the N^{15} 6.33-MeV level, and (c) the N^{15} 7.31-MeV level. Cascade transitions, all in N^{15}, are labeled by the energies of the initial and final levels (in MeV) between which the transitions occur. The 2.8-MeV peak in (a) is due to the $9.06 \rightarrow 6.33$ and $9.16 \rightarrow 6.33$ transitions. Its presence in (a) is due to incomplete separation of the spectra in coincidence with the 5.3- and 6.33-MeV gamma rays.

the observed 2.0-MeV gamma-ray peak. A further contribution arises from the $8.31 \rightarrow 6.33$ cascade [see Fig. 15(b)]; the contribution of this latter transition to Fig. 14(a) is due to incomplete subtraction of the gamma-ray spectrum in coincidence with the 6.33-MeV transition. However, the major fraction of the 2.0-MeV gamma ray apparent in Fig. 14(a) arises from a third source which was found to be due to an O^{15} $7.2 \rightarrow 5.24$ cascade. The $O^{16}+He^3$ gamma-gamma coincidence spectrum was taken to verify this assignment. In order to form the 7.2-MeV state of O^{15} a 6.7-MeV He^{3++} beam was used. The spectrum of low-energy gamma rays in coincidence with the 5.2-MeV doublet is shown in Fig. 17(a). As expected, gamma rays corresponding to the O^{15} $6.85 \rightarrow 5.24$ and $7.2 \rightarrow 5.2$ transitions were observed. It was established that the 2.0-MeV gamma ray is in coincidence with the 5.240-MeV gamma ray primarily rather than the 5.188-MeV gamma ray [Fig. 17(b)]. Thus the measured energy of 2.044 ± 0.007 MeV [Fig. 17(a)] results in an energy of 7.284 ± 0.007 MeV for the sixth-excited state of O^{15}.

The energy of 2.044 ± 0.007 MeV was determined using for calibration annihilation radiation (0.511 MeV), the P^{30} $0.684 \rightarrow 0$ transition following $Si^{28}(He^3,p)$-$S^{30}(\beta^+)P^{30}$, the 1.617-MeV O^{15} $6.857 \rightarrow 5.40$ transition, and the N^{14} $2.31 \rightarrow 0$ transition (2.312 ± 0.0012 MeV[1]) which was in coincidence with a 3.90-MeV gamma ray (i.e., from the N^{14} $6.21 \rightarrow 2.31 \rightarrow 0$ cascade). A limit was set on the possible presence of an O^{15} $7.284 \rightarrow 5.188$ transition by a computer fit to the region of the 2.044-MeV peak [Fig. 17(a)] assuming two peaks separated by 52 keV. The result indicated that, to two standard deviations, the $7.284 \rightarrow 5.188$ transition was <0.1 times as intense as the $7.284 \rightarrow 5.240$ transition.

The available information on branching ratios of the bound excited states of N^{15} is given in Table V. Table VI gives similar information for the states of O^{15} below 9-MeV excitation. In these tables the first three columns list the initial state, final state, and energy of the transition. Following this is the branching ratio information obtained in the present work, information from previous work, and our adopted values using all the available information. The excitation energies of the N^{15} and O^{15} levels in Tables V and VI are taken from Sec. IV.

The branching-ratio information from the present work comes mainly from the (p,γ) and (γ,γ) coincidence measurements and the three-crystal pair spectrometer measurements. However, some information comes from the Li-Ge measurements described in the next section and the magnetic spectrometer studies (Sec. V). The uncertainties due to anisotropies in proton-gamma and gamma-gamma correlations were assumed to be $\lesssim 10\%$. In the proton-gamma correlations the geometrical attenuation coefficients for $P_2(\cos\theta)$ and $P_4(\cos\theta)$ are ~ 0.4 and ~ 0.08, respectively; while for the gamma-

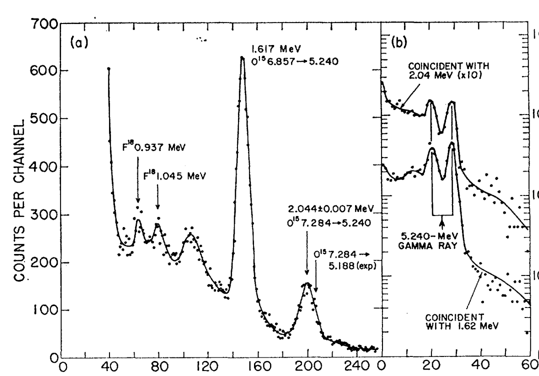

FIG. 17. Gamma-gamma coincidence spectra from $O^{16}+He^3$ at $E_{He^3}=6.7$ MeV. (a) The low-energy gamma rays in coincidence with the 5.2-MeV doublet of O^{15}. The F^{18} peaks are due to accidentals. (b) High-energy gamma rays in coincidence with the 1.617- and 2.044-MeV lines establishing that the latter is in coincidence primarily with the 5.240-MeV gamma ray from the O^{15} $5.240 \rightarrow 0$ transition.

TABLE V. Gamma-ray branching ratios for the gamma-emitting levels of N^{15}.

E_i (MeV)	E_f (MeV)	E_γ (MeV)	Branching ratios (%) a	b	Average
6.323	0	6.323	100[d]	100[d]	100[d]
	5.3[c]	1.02	<1	<3	<1
7.154	0	7.154	<5	···	<5
	5.270	1.884	100	100	100
	5.299	1.855	<10	<5	<5
	6.323	0.831	<0.5	···	<0.5
7.300	0	7.300	98±1	100	98±1
	5.3[c]	2.0	2±1	<10	2±1
	6.323	0.977	<0.25	<3	<0.25
7.563	0	7.563	<2	<3	<2
	5.270	2.293	100	100	100
	5.299	2.264	<5	<20	<5
	6.323	1.240	<0.6	···	<0.6
8.312	0	8.312	80±3	74	78±3
	5.270	3.042	<3	{13	<3
	5.299	3.013	10±2		11±2
	6.323	1.989	7.8±2	13	8.8±2
	7.154	1.158	<1	···	<1
	7.300	1.012	2.2±0.4	⩽6	2.2±0.4
8.570	0	8.570	34±4	29	32±4
	5.270	3.300	63±4	71	65±4
	5.299	3.271	<12	<25	<12
	6.323	2.247	3±1	⩽7	3±1
	7.154	1.416	<5	···	<5
	7.300	1.270	<0.7	···	<0.7
	7.563	1.007	<3	···	<3
9.052	0	9.052	92±3		92±3
	5.3[c]	3.75	3.8±1		3.8±1
	6.323	2.729	3±2		3±2
	7.154	1.898	<10		<10
	7.300	1.752	1.2±0.4		1.2±0.4
	7.563	1.489	<2		<2
	8.312	0.740	<0.5		<0.5
9.155	0	9.155	56±10	18	56±10
	5.270	3.885	{7±3	···	···
	5.299	3.856		10	7±3
	6.323	2.832	10±5	20	10±5
	7.154	2.001	23±5	52	23±5
	7.300	1.855	4±2	···	4±2
	7.563	1.592	<5	···	<5
	8.312	0.843	<0.5	···	<0.5
9.223	0	9.223	<30		<30
	5.270	3.953	<25		<25
	5.299	3.924	100		100
	6.323	2.900	⩽25		⩽25
	7.154	2.069	<30		<30
	7.300	1.923	<30		<30
	7.563	1.660	<20		<20
	8.312	0.911	<5		<5
9.762	0	9.762	100		100
	5.3[c]	4.46	<10		<10
	6.323	3.439	<5		<5
	7.154	2.608	<10		<10
	7.300	2.462	<3		<3
	7.563	2.199	<10		<10
	8.312	1.450	<2		<2
	8.570	1.192	<2		<2
9.832	0	9.832	<30		<30
	5.270	4.562	100		100
	5.299	4.533	<15		<15
	6.323	3.509	<15		<15
	7.154	2.678	<10		<10
	7.300	2.532	<10		<10
	7.563	2.269	<10		<10
9.929	0	9.929	80±10		80±10
	5.3[c]	4.6	10±10		10±10
	6.323	3.606	10±10		10±10
	7.154	2.775	<10		<10
	7.300	2.629	<3		<3
	7.563	2.366	<10		<10
	8.312	1.617	<2		<2
	8.570	1.359	<2		<2
10.074	0	10.074	100		100
	5.3[c]	4.8	<10		<10
	6.323	3.751	<5		<5
	7.154	2.920	<7		<7
	7.300	2.774	<3		<3
	7.563	2.511	<7		<7
	8.312	1.762	<2		<2
	8.570	1.504	<3		<3
10.452	0	10.452	12±12	~17	12±12
	5.3[c]	5.15	72±8	67	72±8
	6.323	4.129	12±8		12±8
	7.154	3.298	<10	~16	<10
	7.300	3.152	4±4		4±4
	7.563	2.889	<10		<10
10.800	0	10.800	55±5	73	60±5
	5.3[c]	5.5	45±5	27	40±5
	6.323	4.477	<5	<4	<4
	7.154	3.646	<5	<4	<4
	7.300	3.500	<5	<4	<4
	7.563	3.237	<7	<4	<4

[a] Present results.
[b] The references for the decay of individual levels are as follows: the 6.323-MeV level through the 8.570-MeV level inclusive, Ref. 8 (preliminary estimates); 9.155 MeV, Ref. 3; 10.452 and 10.800 MeV, Ref. 17.
[c] 5.3 denotes the unresolved 5.270-, 5.299-MeV doublet.
[d] A branching ratio of 100 means that the decay mode in question was the only one observed.

gamma correlations the attenuation factors are ~0.3 and ~0.03, respectively. Thus, in both cases a_4 terms have a negligible effect and a_2 terms of $\sim\pm0.5$ would cause errors of order 10%.

It is seen from Table V that very little systematic quantitative work had been done on the branching ratios of N^{15}. However, there have been some qualitative measurements reported[1,2] in addition to those included in Table V, in particular, an extensive survey[33] of the gamma rays emitted following bombardment of B^{10}, B^{11}, and C^{12} with Li^6 and Li^7. Our branching ratios agree fairly well with previous work except for the N^{15} 9.155-MeV level. Because of the discrepancy between our results and the preliminary results[3] from $N^{14}(n,\gamma)N^{15}$ we have not averaged our results with this previous work.

[33] E. Norbeck, S. A. Coon, R. R. Carlson, and E. Berkowitz, Phys. Rev. 130, 1971 (1963).

IV. LITHIUM-DRIFTED GERMANIUM SPECTRA

As a part of the study of gamma-ray transitions in N^{15} and O^{15} gamma-ray spectra were recorded following deuteron bombardment of ZrN and C^{14} targets and

TABLE VI. Gamma-ray branching ratios for O^{15}.

E_i (MeV)	E_f (MeV)	E_γ (MeV)	Branching ratio (%)[a]
6.180	0	6.180	100[b]
	5.188	0.992	<2.5
	5.240	0.940	<2.5
6.789	0	6.789	100
	5.188	1.601	<6
	5.240	1.549	<6
	6.180	0.609	<7
6.857	0	6.857	<10
	5.188	1.669	<15
	5.240	1.617	100
	6.180	0.677	<0.4
7.284	0	7.284	<30
	5.188	2.096	<10
	5.240	2.044	100
	6.180	1.104	<2
7.550	0	7.550	3.3±0.3
	5.188	2.362	17±1
	5.240	2.310	<4.3
	6.180	1.370	57±1
	6.789	0.761	22.7±1
	6.857	0.693	<5.5
8.283	0	8.283	55
	5.188	3.095	...
	5.240	3.043	40
	6.180	2.103	4
	6.789	1.494	...
	6.857	1.426	1
	7.284	0.999	<1
8.735	0	8.735	...
	5.188	3.547	67
	5.240	3.495	...
	6.180	2.555	33
	6.789	1.946	...
	6.857	1.878	...
8.915	0	8.915	21
	5.188	3.727	23
	5.240	3.675	...
	6.180	2.735	30
	6.789	2.126	...
	6.857	2.058	26
8.980	0	8.980	93
	5.188	3.792	6
	5.240	3.740	...
	6.180	2.800	(0.25)
	6.789	2.191	(0.5)
	6.857	2.123	...

[a] Present results for the bound levels of O^{15} and, for the unbound levels, an average of the measurements reported in the following: T. Tabata and K. Okano, J. Phys. Soc. Japan **15**, 1552 (1960); D. F. Hebbard and G. M. Bailey, Nucl. Phys. **49**, 666 (1963); B. Povh and D. F. Hebbard, Phys. Rev. **115**, 608 (1959); D. F. Hebbard and B. Povh, Nucl. Phys. **13**, 642 (1959); S. Bashkin, R. R. Carlson, and E. B. Nelson, Phys. Rev. **99**, 107 (1955); A. E. Evans and J. B. Marion, Bull. Am. Phys. Soc. **10**, 37 (1965) and A. E. Evans, Ph.D. thesis, University of Maryland, 1965 (unpublished).
[b] A branching ratio of 100 means that the decay mode in question was the only one observed.

He^3 bombardment of quartz (SiO_2) and $C^{12,13}$ targets using a lithium-drifted germanium gamma-ray detector having a sensitive volume of 3 cm^3. The part of this work bearing on the 5-MeV doublets in N^{15} and O^{15} has already been reported.[4]

Before considering these results it is advantageous to review the information concerning the excitation energies of the bound N^{15} states. By far the most accurate determination of the excitation energies of the N^{15} 5.3-MeV doublet comes from the $N^{14}(n,\gamma)N^{15}$ measurements of Carter and Motz.[3] Their results gave 5.298±0.001 and 5.269±0.001 MeV for the excitation energies of these two levels, 28.8±0.2 keV for the separation between them and 10.8323±0.0015 MeV for the Q value of the $N^{15}(n,\gamma)N^{15}$ reaction. The adjusted $N^{14}(n,\gamma)N^{15}$ Q value from Everling *et al.*[34] is 10.8343±0.0009 MeV, 2 keV higher than the value of Carter and Motz, and the average excitation energy of the N^{15} 5.30-MeV level from $N^{14}(d,p)N^{15}$, and $C^{15}(\beta)N^{15}$ measurements[6,10,11,35] is 5.3016±0.003 MeV, 3.6 keV higher than the $N^{14}(n,\gamma)N^{15}$ result. For these reasons we adopt 5.299±0.001 and 5.270±0.001 MeV for the excitation energies of the 5.3-MeV doublet of N^{15}.

Excitation energies of the other bound levels of N^{15} up to and including the 9.16-MeV level can be obtained from the $N^{14}(n,\gamma)N^{15}$ work of Carter and Motz[3] and the separation energies between levels quoted by Sperduto *et al.*[36] and Douglas *et al.*[37] Excitation energies can be obtained from the gamma-ray measurements of Carter and Motz for all of the lowest ten excited states of N^{15} save the 7.57-, 8.57-, and 9.06-MeV levels. These authors quote gamma-ray energies to 0.1% except for the 5.3-MeV doublet, already considered, and the fifth-excited state for which they quote 7.300±0.0015 MeV. We use this latter value together with the separation energies from the $N^{14}(d,p)N^{15*}$ measurements[36,37] to obtain excitation energies for the 7.57- and 8.57-MeV levels. Likewise, we obtain the excitation energies of the 9.06-, and 9.23-MeV levels from the excitation energy of the 9.16-MeV level derived from the $N^{14}(n,\gamma)$-N^{15} work[3] and the difference in energies between the 9.16-MeV level and the 9.06- and 9.23-MeV levels quoted by Sperduto *et al.*[36] and Kashy.[6] The excitation energies listed in Table VII for the N^{15} levels below 9.5 MeV were obtained by this procedure.

TABLE VII. Excitation energies of N^{15} levels.[a]

Excitation energy (MeV)	Uncertainty (keV)
5.270	1
5.299	1
6.323	3.6
7.154	2.0
7.300	1.5
7.563	1.8
8.312	2.0
8.570	2.1
9.052	4.6
9.155	2.3
9.223	6.0
9.762	3.6
9.832	7.0
9.929	3.6
10.074	4.5

[a] From Refs. 3, 6, 35, 36, and 37.

[34] F. Everling, L. A. Konig, J. H. E. Mattauch, and A. H. Wapstra, Nucl. Phys. **15**, 342 (1960).
[35] R. Malm and W. W. Buechner, Phys. Rev. **80**, 771 (1950).
[36] A. Sperduto, W. W. Buechner, C. K. Bockelman, and C. P. Browne, Phys. Rev. **96**, 1316 (1954).
[37] R. A. Douglas, J. W. Broer, R. Chiba, D. F. Herring, and A. E. Silverstein, Phys. Rev. **104**, 1059 (1956).

We note than an accurate experimental value for the Q value of the $N^{14}(d,p)N^{15}$ reaction can be obtained by combining the excitation energy quoted by Motz and Carter[3] for the 7.31-MeV level of N^{15} with the Q-value determination of Douglas *et al.*[36] for this level in the $N^{14}(d,p)N^{15}$ reaction. The result is 8.608 ± 0.0018 MeV as compared to the value of 8.6096 ± 0.0008 MeV quoted as the least-squares adjusted $N^{14}(d,p)N^{15}$ Q value by Everling *et al.*[34] The Q value for the ground state $C^{14}(d,n)N^{15}$ reaction is most accurately determined from the Q value for the $C^{14}(p,n)N^{14}$ reaction[38] ($Q=-0.6264\pm0.0005$ MeV) and the Q value for the $N^{14}(d,p)N^{15}$ reaction ($Q=8.608\pm0.0018$ MeV), which give 7.9816 ± 0.0019 MeV for the $C^{14}(d,n)N^{15}$ Q value. Combining this ground state Q value with the threshold measurements of Chiba[5] gives the excitation energies quoted in Table VII for the N^{15} 9.77-, 9.94-, and 10.06-MeV levels. The excitation energy of the 9.83-MeV level is obtained from an average of the results of Sperduto *et al.*[36] and Chiba.[5] The excitation energies listed in Table VII will be used in the remainder of this report.

Representative Li-Ge spectra from $C^{14}+d$, $N^{14}+d$, and $C^{12,13}+He^3$ are shown in Figs. 18, 19, and 20, respectively. These and all other Li-Ge spectra recorded in this study were obtained with the detector placed 15 cm from the target at 90° to the incident beam. For this geometrical arrangement the uncertainties in the measurements of gamma-ray energies due to Doppler effects are small compared to other errors. The identifications of the lines which are made in Figs. 18, 19, and 20 were made straightforwardly on the basis of the results reported in other sections of this paper and from internal energy calibrations.

As an example of the type of information obtained from the Li-Ge spectra we give in Table VIII a summary of the major part of the information obtained from the $N^{14}+d$ Li-Ge spectra. In the first two columns of Table VIII are listed the $N^{14}+d$ gamma rays positively identified and their assignments. The third column lists the excitation energies of the initial states based on energies of 5.299 ± 0.001 MeV and 5.270 ± 0.001 MeV for the N^{15} doublet and 5.240 ± 0.0013 MeV for the second-excited state of O^{15}. The latter energy was obtained relative to the N^{15} 5.270-MeV line from the $N^{14}+d$ spectra.[4] In the fourth column is listed the observed full width at half-maximum of the peaks corrected for the detector resolution which varied from 6.0 ± 0.4 keV for the O^{17} 0.87-MeV line to 10.5 ± 1 keV for the N^{15} 5.270-MeV two-escape peak. The maximum width allowed by the kinematics is listed in column five, i.e., the width which would be observed if all gamma rays were emitted at 90° to the beam and the lifetimes of the emitting states were very short compared to the stopping time of the recoiling nuclei. For all five of the observed cascades to the 5-MeV doublet of N^{15} or O^{15}

[38] R. Sanders, Phys. Rev. **104**, 1434 (1956).

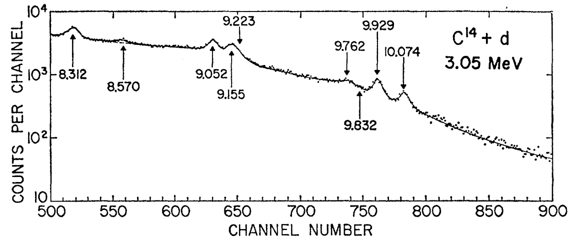

FIG. 18. Partial Li-Ge two-escape peak gamma-ray spectra from $C^{14}(d,n\gamma)N^{15}$ at $E_d=3.05$ MeV and $\theta_\gamma=90°$. The resolution of the detector for the two-escape peaks is about 11 keV and the dispersion is about 7 keV/channel. The peaks correspond to ground-state transitions in N^{15} and are labeled by the excitation energies (in MeV) of the initial states (following Table VII). The important information obtained from this spectrum is the relative intensities of the various lines and the fact that all the observed lines are Doppler broadened.

a cascade was observed to only one member of the doublet. The limit on the relative intensity (I_R) of the cascade to the other member of the doublet is given in the last column of Table VIII. The gamma-ray energies given in parenthesis in the first column of Table VIII were taken from Table VII and were used for calibration lines. The information obtained for the first- and second-excited states of N^{15} and O^{15} has already been reported.[4]

The information given in Table VIII comes from the spectrum of Fig. 19 and from spectra covering the energy range up to channel 400 and from channels 400 to 680 with dispersions of 2.5 and 3 keV/channel, respectively.

The excitation energies of the N^{15} levels listed in Table VIII are in excellent agreement with those of Table VII. The excitation energy of 6.857 ± 0.0032 MeV obtained for the fifth-excited state of O^{15} is in good agreement with the best previous determination of 6.860 ± 0.009 MeV.[39] Combining the value of 6.857 ±0.0032 MeV with the energy separation[39] of 68 ± 5.7 keV between the O^{15} 6.86- and 6.79-MeV levels gives 6.789 ± 0.0065 for the excitation energy of the latter. The excitation energy of the third excited state of O^{15} was obtained from an energy measurement of its ground-state transition relative to nearby lines of N^{15} and O^{15}. It is seen from Table VIII that the O^{15} 7.284$\rightarrow$ 5.240 transition observed in a gamma-gamma coincidence spectrum is also observable in the $N^{14}+d$ Li-Ge spectra; of course, the identification of this line in the Li-Ge spectra is based on the evidence from the gamma-gamma coincidence work.

The information obtained from the Li-Ge spectra from $C^{14}+d$ and $C^{13}+He^3$ is similar to that given in Table VIII. The excitation energies of the levels of O^{15} below 9-MeV excitation from this and previous work are listed in Table IX. The information obtained from the Li-Ge spectra bearing on the branching ratios of

[39] J. B. Marion, R. M. Brugger, and T. W. Bonner, Phys. Rev. **100**, 46 (1955).

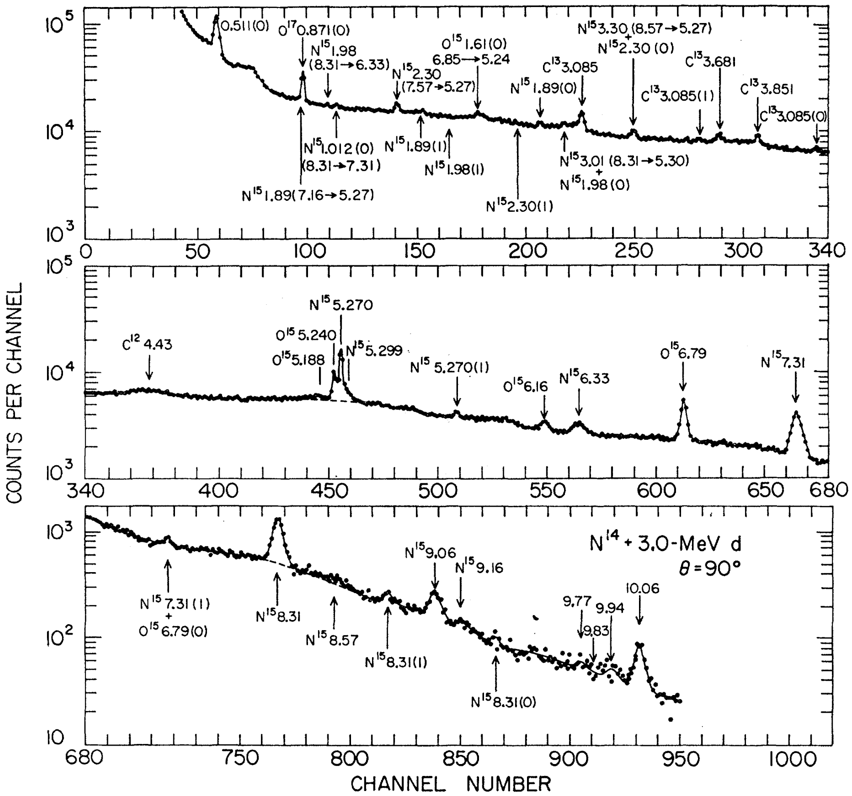

FIG. 19. Li-Ge gamma-ray survey spectrum from $N^{14}+d$ at $E_d=3.0$ MeV and $\theta_\gamma=90°$. The resolution of the detector varies from 6.0 ± 0.4 keV at 0.870 MeV to about 11 keV for a 10-MeV two-escape peak and the dispersion is about 10 keV/channel. For channels greater than 260 all the labeled peaks correspond to ground-state transitions and are identified by the nucleus and nominal excitation energy (in MeV) of the initial state to which they correspond. Most prominent peaks are two-escape peaks; one-escape peaks are labeled by (1) and full-energy peaks by (0). For channels below 260 most of the peaks arise from cascade transitions. The two-escape peaks or the full-energy peaks of cascade transitions are labeled by the nucleus to which they are assigned, the transition energy (in MeV), and the excitation energies (in MeV) of the initial and final states between which the transitions occur. The C^{13} and O^{17} peaks arise from the contaminant reactions $C^{12}(d,p\gamma)C^{13}$ and $O^{16}(d,p\gamma)O^{17}$. The solid curve drawn in the region between channels 870 and 950 is a computer fit assuming three Gaussian peaks superimposed on an exponential background. This fit gives evidence for the peaks marked 9.77 and 9.94 and is consistent with the absence of a peak at the position marked 9.83. Other spectra were taken at higher dispersion to investigate the pulse-height region below channel 680 in more detail.

the bound levels of N^{15} and O^{15} has been incorporated into Tables V and VI.

Gamma-ray transitions originating from all the bound levels of N^{15} and O^{15} were observed in at least one Li-Ge spectrum and all the lines were found to be Doppler broadened except those originating from the N^{15} 5.270- and O^{15} 5.240-MeV levels.[4] Thus, all the bound N^{15} and O^{15} levels except these latter two have lifetimes shorter than, or comparable to, the stopping time of the recoiling N^{15} and O^{15} nuclei in the various targets used. All the linewidths were consistent with lifetimes negligibly short compared to the stopping time as are those listed in Table VIII. We take 5×10^{-13} sec as a conservative estimate of the slowing down time of the recoiling nuclei[28] and thus set a limit of $\tau \lesssim 5\times10^{-13}$ sec for the mean lifetimes of all the bound levels of N^{15} and O^{15} except the N^{15} 5.270- and O^{15} 5.240-MeV levels. These limits will be useful in setting limits on possible spin-parity assignments.

TABLE VIII. Results for gamma-ray transitions in N^{15} and O^{15} observed with a Li-Ge detector from $N^{14}+d$ at $E_d=3.0$ MeV.

E_γ (MeV)	Assignment	E_i (MeV)	Δ_{obs} (keV)	Δ_{max} (keV)	I_R
1.617 ± 0.003	O^{15} 6.860 → 5.240	6.857 ± 0.0032	9 ± 3	10	<0.15
1.883 ± 0.003	N^{15} 7.154 → 5.270	7.153 ± 0.0032	16 ± 3	23	<0.10
1.991 ± 0.005	N^{15} 8.312 → 6.323	···	17 ± 6	20	···
2.045 ± 0.006	O^{15} 7.284 → 5.240	7.285 ± 0.006	15 ± 5	13	···
2.294 ± 0.003	N^{15} 7.563 → 5.270	7.564 ± 0.0032	16 ± 2	26	<0.05
3.010 ± 0.004	N^{15} 8.312 → 5.299	8.309 ± 0.0041	15 ± 6	30	<0.3
3.303 ± 0.003	N^{15} 8.570 → 5.270	8.573 ± 0.0032	25 ± 3	32	<0.18
6.180 ± 0.004	O^{15} 6.180 → 0	6.180 ± 0.004	42 ± 8	46	···
(6.323)	N^{15} 6.323 → 0		64 ± 9	84	···
(6.791)	O^{15} 6.791 → 0		31 ± 2	39	···
(7.300)	N^{15} 7.300 → 0		55 ± 5	87	···
(8.312)	N^{15} 8.312 → 0		50 ± 5	85	···
(8.570)	N^{15} 8.570 → 0		49 ± 8	84	···
(9.052)	N^{15} 9.052 → 0		60 ± 6	71	···
(9.155)	N^{15} 9.155 → 0		62 ± 10	70	···
(10.074)	N^{15} 10.074 → 0		55 ± 7	65	···

V. MAGNETIC-SPECTROMETER MEASUREMENTS

A. The Spectra of Internal Pairs

Selected portions of the spectra of internal pairs emitted from $N^{14}+d$ and $C^{14}+d$ were studied using the Brookhaven magnetic-lens intermediate-image spectrometer.[40] In general, the spectra were similar to those obtained with the three-crystal pair spectrometer except for the better resolution obtained with the magnetic spectrometer. The yields from $O^{16}+He^3$ and $C^{13}+He^3$ were quite low at the He^3 energies available (compare the intensity scales of Figs. 1–4) so that the internal pairs from these two reactions were not studied. The O^{15} positron activity gave rise to an intense background for low-energy transitions ($\lesssim 4$ MeV) for $N^{14}+d$ and the C^{15} beta activity gave rise to a strong background peaking near a transition energy of 6 MeV.

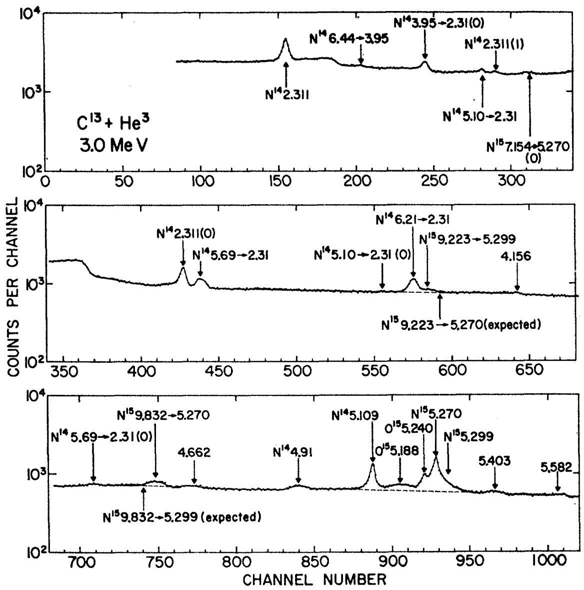

FIG. 20. Partial Li-Ge gamma-ray spectrum from $C^{12,13}+He^3$ at $E_{He^3}=3.0$ MeV and $\theta_\gamma=90°$. The resolution of the detector varies with gamma-ray energy from about 7 keV to about 11 keV over the energy region shown and the dispersion is about 3.5 keV/channel. Identified peaks are labeled by the nucleus to which they correspond and if one-escape or full-energy peaks by (1) or (0), respectively. The N^{14} peaks arise from the $C^{12}(He^3,p\gamma)N^{14}$ reaction, the N^{15} and O^{15} peaks from $C^{13}+He^3$. Cascade transitions are labeled by the excitation energies (in MeV) of the initial and final levels between which they occur and ground-state transitions are labeled by the excitation energy (in MeV) of the initial state. Unidentified peaks are labeled by their energies (in MeV) only, on the assumption that they are two-escape peaks. The most important information obtained from this spectrum is that the N^{15} 9.223- and 9.832-MeV levels decay to the upper and lower members of the 5.3-MeV doublet, respectively, and both cascade transitions are Doppler broadened.

These backgrounds were severe enough to preclude the study of cascade transitions in N^{15} and O^{15} since these were either too weak or of too low an energy. However, the more intense ground-state transitions emitted from $N^{14}+d$ were easily studied with the exception of the O^{15} 6.18 → 0 transition which was obscured by the relatively intense $E0$ O^{16} 6.06 → 0 line due to the $N^{15}(d,n)O^{16}$ reaction. Transitions arising from $C^{14}+d$ were studied using deuteron bombarding energies

[40] D. E. Alburger, Rev. Sci. Instr. **27**, 991 (1956); Phys. Rev. **111**, 1586 (1958); **118**, 235 (1960).

TABLE IX. Excitation energies of O^{15} levels.[a]

Excitation energy[b] (MeV)	Uncertainty (keV)
5.188	6.0
5.240	1.3
6.180	4.0
6.789	6.5
6.857	3.2
7.284	7.0
7.550	2.2
8.283	3.0
8.735	6.0
8.915	3.0
8.980	3.0

[a] From present results and Refs. 4, 39, and 26.
[b] The level energies of the unbound levels are based on the averages of the resonant energies for the $N^{14}(p,p)N^{14}$ and $N^{14}(p,\gamma)O^{15}$ reactions compiled by Evans (Ref. 26) and on a proton binding energy in O^{15} of 7.2910 ± 0.0023 MeV which is obtained from the $N^{14}(d,p)N^{15}$ Q value given in this report, the binding energy of the deuteron and the Q value for the $N^{15}(p,n)O^{15}$ reaction of -3.5418 ± 0.0014 MeV [Ref. 26 and K. W. Jones, L. Lidofsky, and J. W. Weil, Phys. Rev. **112**, 1252 (1958)].

selected to give the best conditions of yield to background for each pair line studied.

The targets used in this work were similar to those used in the three-crystal pair spectrometer measurements except that the N^{14} target was prepared on a 0.05 mil Ni foil. Two of the partial spectra are illustrated in Figs. 21 and 22.

B. Internal-Pair Correlation Measurements

The utilization of the intermediate-image spectrometer for determining the multipolarity of electromagnetic transitions between nuclear states has been described in some detail previously.[41] Briefly, the method is to measure the pair-line yield with a baffle in place (Y_{in}) to the yield without the baffle in place (Y_{out}) and then compare the ratio $R_\omega'=Y_{in}/Y_{out}$ for a particular pair line to theoretical curves for various multipolarities. The factor R_ω is obtained from R_ω' by

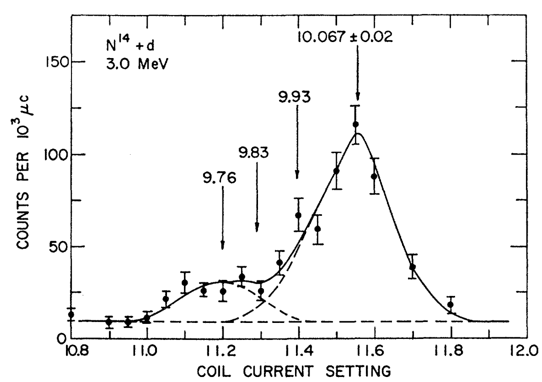

FIG. 21. Partial spectrum of internal-pair lines from levels of N^{15} populated by 3.0-MeV deuteron bombardment of a N^{14} target, indicating the presence of the transitions 9.76 → 0 and 10.07 → 0 and the expected positions of the 9.83 → 0 and 9.93 → 0 transitions. The energy calibration was made relative to the 9.052 → 0 ransition of N^{15}.

[41] E. K. Warburton, D. E. Alburger, A. Gallmann, P. Wagner, and L. F. Chase, Jr., Phys. Rev. **133**, B42 (1964).

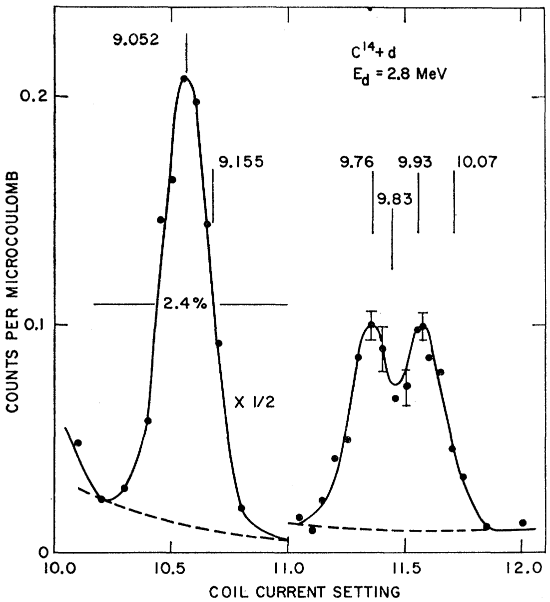

FIG. 22. Partial spectrum of internal-pair lines from levels of N^{15} populated by 2.8-MeV deuteron bombardment of a C^{14} target indicating the presence of the $9.052 \rightarrow 0$, $9.76 \rightarrow 0$, and $9.93 \rightarrow 0$ transitions and the expected positions of the $9.115 \rightarrow 0$, $9.83 \rightarrow 0$, and $10.07 \rightarrow 0$ transitions.

correcting for the alignment of the emitting level.[41] Curves of R_ω versus transition energy are shown in Fig. 23. The open circles in this figure are measurements of R_ω for calibration lines while the closed circles represent the transitions in N^{15} and O^{15} listed in Table X. Figure 23 is similar to one given in a report[29] of studies of transitions in B^{11} and C^{11} except that it has been extended to transition energies of 11 MeV and all

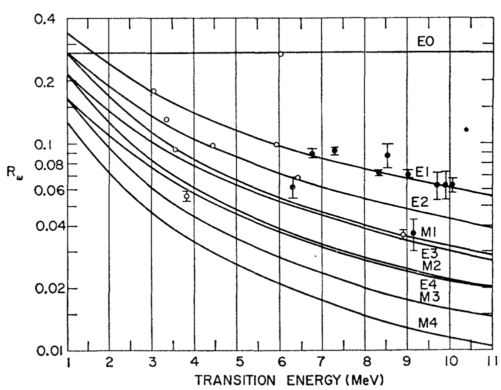

FIG. 23. Experimentally measured ratios R_ω plotted as functions of internal-pair transition energies. The open circles present the results of calibration measurements for transitions of known multipolarity (Ref. 29) while the curves show the normalized theoretical values calculated for transitions of multipole order ranging from $E0$ to $M4$ (Ref. 29). The results of the present measurements for transitions in N^{15} and O^{15}, as summarized in Table X, are shown by the solid circles. The designation of eight of these transitions as being $E1$ in character is readily suggested by the correspondence between the measured values and the calculated $E1$ curve.

the B^{11} and C^{11} transitions have been omitted with the exception of the B^{11} $M1$ $8.92 \rightarrow 0$ transition which has been retained as a calibration line.

The measurements for the majority of the transitions listed in Table X were straightforward and were performed with the maximum transmission of the spectrometer which corresponds to about 3% resolution (full width at half-maximum) for the pair lines. However, the N^{15} $9.16 \rightarrow 0$ transition was studied at a resolution of 1.8% in order to separate it from the $9.05 \rightarrow 0$ transition and the N^{15} $9.76 \rightarrow 0$ and $9.93 \rightarrow 0$ transitions were studied at a resolution of 2.4% (Fig. 22). Note that the relative intensities of the 9.76-, 9.94-, and 10.07-MeV ground-state transitions change markedly between $E_d = 2.8$ MeV (Fig. 22) and 3.05-MeV (Fig. 18). The reactions used to populate the levels and the bombarding energies used are listed in Table X.

As in previous work, identification of $E1$ transitions is straightforward and is uncomplicated by the effects of nuclear alignment. Of the ten transitions studied,

TABLE X. Summary of the experimental ratios R_ω' for ground-state transitions in N^{15} and O^{15}.

Initial state (MeV)	Reaction, E_d (MeV)	R_ω'	Multi-polarity	Spin-parity
N^{15} 6.323	$C^{14}+d$, 1.9	0.061±0.007	$M1$, $E2$	$\frac{3}{2}^-$
O^{15} 6.789	$N^{14}+d$, 3.0	0.088±0.005	$E1$	$\frac{3}{2}^+$
N^{15} 7.300	$N^{14}+d$, 3.0	0.091±0.003	$E1$	$\frac{3}{2}^+$
N^{15} 8.312	$N^{14}+d$, 3.0	0.071±0.002	$E1$	$\frac{1}{2}^+$, $(\frac{3}{2}^+)$
N^{15} 8.570	$C^{14}+d$, 3.4	0.086±0.011	$E1$	$\frac{3}{2}^+$
N^{15} 9.052	$N^{14}+d$, 3.2	0.070±0.003	$E1$	$\frac{1}{2}^+$, $\frac{3}{2}^+$
N^{15} 9.155	$C^{14}+d$, 3.4	0.036±0.006	$(M1)$	$(\frac{1}{2}^-, \frac{3}{2}^-)$
N^{15} 9.762	$C^{14}+d$, 2.8	0.062±0.009	$(E1)$	$(\frac{1}{2}^+, \frac{3}{2}^+)$
N^{15} 9.929	$C^{14}+d$, 2.8	0.062±0.009	$(E1)$	$(\frac{1}{2}^+, \frac{3}{2}^+)$
N^{15} 10.074	$N^{14}+d$, 3.2	0.062±0.005	$E1$	$\frac{1}{2}^+$, $\frac{3}{2}^+$

eight were found to be $E1$; the remaining two are the $6.32 \rightarrow 0$ and $9.16 \rightarrow 0$ transitions in N^{15}. The N^{15} $6.32 \rightarrow 0$ transition is known to be an $M1$, $E2$ mixture with an amplitude ratio x of $E2$ to $M1$ radiation of $+(0.09_{-0.03}^{+0.06})$ or $+(1.4_{-0.4}^{+0.1})$.[9] It was hoped that a measurement of R_ω' would eliminate one of these possibilities; however, the $6.32 \rightarrow 0$ transition has a nonisotropic angular distribution for the conditions used (see Table II) and it turned out that the alignment correction for the observed angular distribution was such that the theoretical values of R_ω for the two different values of x were practically indistinguishable. In other words, for $x = +0.09$ R_ω' is predicted to be 0.057 and for $x = 1.4$ R_ω' is predicted to be 0.062; while the experimentally observed value of R_ω' was 0.061 ± 0.007. We note that it would be quite possible to distinguish between the two possible values of x if experimental conditions were found such that the angular distribution of the $6.32 \rightarrow 0$ transition had a negative value of a_2 rather than a positive value (Table

II) since in this case the alignment corrections for the two values of x would be in opposite directions.

The measurement of R_ω' for the N^{15} $9.16 \rightarrow 0$ transition indicates that this transition is probably $M1$ and is certainly not pure $E1$; however, the angular distribution of this transition was not measured so there is an uncertainty from the possible effects of alignment in addition to the relatively large statistical uncertainties. Thus, multipolarities other than $M1$ must be considered. We return to a consideration of this transition in the next section.

VI. DISCUSSION

A. Synthesis with Previous Results

Our final conclusions regarding the gamma-ray decay schemes of the bound levels of N^{15} and the O^{15} levels below an excitation energy of 9 MeV are collected in Figs. 24 and 25. The gamma-ray branching ratios are taken from Tables V and VI. The spin-parity assignments are obtained by combining previous work (Fig. 1) with the evidence presented in this paper, the interpretation of which we shall now discuss level by level. In this discussion we shall emphasize the identification of mirror levels in N^{15} and O^{15} using as evidence relative excitation energies, spin-parity information, nucleon reduced widths, and gamma-ray decay schemes. For the latter we make use of the work of Morpurgo[42] which shows that dipole transition strengths for analogous transitions in mirror nuclei are expected to be quite nearly equal.

The First and Second Excited States of N^{15} and O^{15}

We have no new information to add for these two levels. We note that the level order of the first two levels in N^{15} is inverted in O^{15}. This should be kept in mind when discussing gamma-ray transitions to these states from higher levels.

The N^{15} 6.323- and O^{15} 6.180-MeV Levels

We consider that the evidence that these two levels form a mirror pair is quite conclusive even though the parity of the O^{15} 6.180-MeV level has not been determined rigorously. Our upper limit of 1% (Table V) for the branching ratio of the N^{15} 6.323-MeV level to the 5.3-MeV doublet of N^{15} is approaching the region of interest. The $E1$ transitions to these doublets are retarded by an $E_\gamma{}^3$ energy factor of $\sim 4\times 10^{-3}$ relative to the $M1$ ground-state transition. Since $E1$ transitions are, on the average, stronger than $M1$ transitions by about a factor of seven[43] the branch to the doublet would therefore be expected *a priori* to be greater than 1%.

[42] G. Morpurgo, Phys. Rev. **114**, 1075 (1959).

[43] D. H. Wilkinson, in *Nuclear Spectroscopy*, Part B, edited by F. Ajzenberg-Selove (Academic Press Inc., New York, 1960), Part B, p. 852ff.

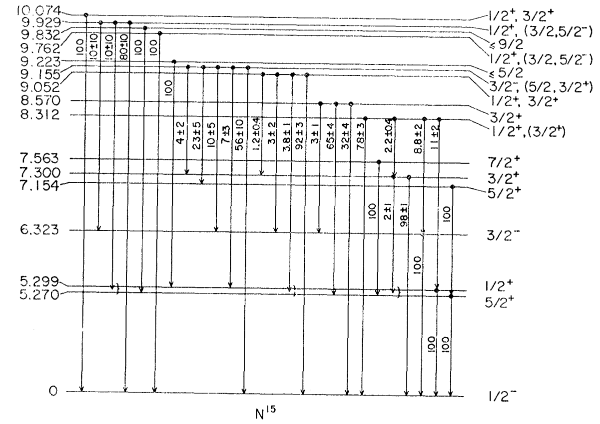

FIG. 24. Level scheme of N^{15} showing spins, parities and decay modes of the bound levels. The various assignments and branching ratios are obtained as a synthesis of the results of this experiment with those reported from other sources, as explained in the text. Uncertain or less likely assignments are enclosed in parentheses.

The N^{15} 7.300- and O^{15} 6.789-MeV Levels

Previous evidence that these two levels form a mirror pair was quite conclusive. We have verified that both levels decay by $E1$ transitions to their respective ground states and have obtained firmer limits for the strengths of possible cascades to the third-excited states for both. The branching ratio of 2% (Table V) found for the cascade from the N^{15} 7.300-MeV level to the 5.3-MeV doublet seems a reasonable value and is consistent with our upper limit of 6% (Table VI) for the branching ratio of the O^{15} 6.789-MeV level to either the 5.188- or 5.240-MeV level of O^{15}.

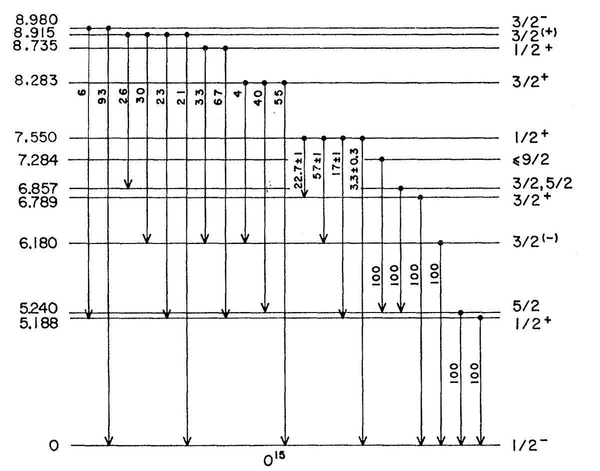

FIG. 25. Level scheme of O^{15} showing spins, parities and decay modes of the levels below an excitation energy of 9 MeV. The various assignments and branching ratios are obtained as a synthesis of the results of this experiment with those reported from other sources, as explained in the text. Uncertain or less likely assignments are enclosed in parentheses.

The N^{15} 7.154- and O^{15} 6.857-MeV Levels

These levels almost certainly form a mirror pair, and this we shall assume in the following discussion. We have established that the N^{15} $7.154 \rightarrow 5.270$ cascade is at least ten times as intense as the $7.154 \rightarrow 5.299$ cascade, and that the O^{15} $6.857 \rightarrow 5.240$ cascade is at least 6.7 times as intense as the O^{15} $6.857 \rightarrow 5.188$ cascade. Thus, each of the levels under consideration decays primarily to the $J=\frac{5}{2}$ member of the 5.3-MeV doublet of N^{15} and O^{15}, respectively.

Our lifetime limit of $\tau < 5\times10^{-13}$ sec establishes the O^{15} $6.857 \rightarrow 5.240$ transition to be dipole since this limit corresponds to Weisskopf estimates[43] which are at least 66 and 1320 times the single-particle speeds for $E2$ and $M2$ radiations, respectively, which are unrealistically large for $A=15$.[43] The establishment of the dipole character of this cascade restricts the O^{15} 6.857-MeV level to $J=\frac{3}{2}$, $\frac{5}{2}$, or $\frac{7}{2}$, and since $J\leqslant\frac{5}{2}$ from previous work (Fig. 1), we have $J=\frac{3}{2}$ or $\frac{5}{2}$ for the O^{15} 6.857-MeV level.

The N^{15} 7.563- and O^{15} 7.284-MeV Levels

Both of these levels decay primarily to the $J=\frac{5}{2}$ member of the 5.3-MeV doublet. We have observed no other transition from either level and have set limits (Tables V and VI) on the relative intensities of other transitions. From their relative excitation energies (Fig. 1) and the similarity of their decay modes, it appears that these two levels almost certainly form a mirror pair—in which case they both have $J^{\pi}=\frac{7}{2}^{+}$. Evidence against this has been presented by Hebbard and Povh[44] who reported transitions to an O^{15} level at an excitation energy of 7.16 ± 0.05 MeV from the $\frac{3}{2}^{+}$ 8.283-MeV level and the $\frac{1}{2}^{+}$ 8.735-MeV level (uncertain). The reported strength of the first of these was large enough that it must be dipole. (The strength reported for the $8.283 \rightarrow 7.16$ transition would correspond to $\sim$400 Weisskopf units[43] if $E2$.) This, in fact, constituted the first evidence for an O^{15} level near 7.2-MeV excitation. However, this evidence[44] does not appear to be conclusive and was not confirmed in the recent $N^{14}(p,\gamma)O^{15}$ work of Evans and Marion.[26] The presence of an O^{15} level near an excitation energy of 7.2 MeV has since been confirmed using the $N^{14}(d,n)O^{15}$ reaction.[26] We find an excitation energy of 7.284 ± 0.007 MeV for the sixth excited state of O^{15}—interestingly close to the proton binding energy of 7.2910 ± 0.0023 MeV (see footnote for Table IX). This excitation energy is sufficiently removed from the previous value of 7.16 ± 0.05 MeV[44] to cast further doubt on the presence of the cascades O^{15} $8.283 \rightarrow 7.284$ and $8.735 \rightarrow 7.284$. The lifetime limit, $\tau<5\times10^{-13}$ sec, restricts the O^{15} $7.284 \rightarrow 5.240$ transition to be dipole or $E2$ (unlikely) radiation. Thus, the O^{15} 7.284-MeV level has $J\leqslant\frac{9}{2}$ if the parity is even and $J=\frac{3}{2}$, $\frac{5}{2}$, or $\frac{7}{2}$ if the parity is odd.

The neutron angular distribution of the reaction $N^{14}(d,n)O^{15}$ (7.284-MeV level) has been measured[25] at $E_d=3.564$ MeV. The data was fitted by the plane-wave stripping theory with corrections for Coulomb effects of the incident deuteron. The best fit was obtained[25] for $l_p=2$ and thus $J^{\pi}\leqslant\frac{7}{2}^{+}$. However, the fit was not good and the plane-wave theory is not valid for a level so close to the proton binding energy. Thus, we do not feel a preference for even parity for the O^{15} 7.284-MeV level is indicated from this source.

[44] D. F. Hebbard and B. Povh, Nucl. Phys. **13**, 642 (1959).

The N^{15} 8.312- and O^{15} 7.550-MeV Levels

The evidence that these two levels form a mirror pair is that both have s-wave nucleon widths close to the single-particle value,[15,16,26] and there is no other known level in N^{15} below an excitation energy of 9 MeV which could be the mirror of the $J^{\pi}=\frac{1}{2}^{+}$ O^{15} 7.550-MeV level.

As indicated in Fig. 1 the N^{15} 8.31-MeV level is probably $J^{\pi}=\frac{1}{2}^{+}$. If, however, it has $J^{\pi}=\frac{3}{2}^{+}$ then the internal pair correlation measurement on the N^{15} $8.31 \rightarrow 0$ transition chooses the alternative $x=-(0.16\pm0.09)$ for the $E1$, $M2$ mixing ratio of this transition—$x=-(0.16\pm0.09)$ or $+(2.9\pm0.9)$ being allowed by previous angular correlation measurements.[9]

Morpurgo[42] has shown that if charge symmetry is obeyed and Coulomb interactions are neglected then $E1$ transition rates for transitions between analog states in mirror nuclei are identically equal, while the strengths of $M1$ transitions should not differ by more than a factor of 1.5. These expectations are grossly violated for the mirror pair under consideration. This is illustrated by the transition strengths given in Table XI for the decays of the N^{15} 8.312- and O^{15} 7.550-MeV levels to the first $\frac{1}{2}^{-}$, $\frac{1}{2}^{+}$, $\frac{3}{2}^{-}$, and $\frac{3}{2}^{+}$ states of N^{15} and O^{15}. In the first two columns of this table are listed the spin-parity of the state to which the transition occurs and the assumed multipolarity of the transitions from these $J^{\pi}=\frac{1}{2}^{+}$ states. In the third and fourth columns are listed the radiative widths for the O^{15} transitions and the transition strengths in Weisskopf units.[43] The total radiative width of the N^{15} 8.321-MeV level is not known so that the transition strengths for the decay of this level, given in the fifth column, are normalized assuming that the N^{15} $8.312 \rightarrow 7.300$ and O^{15} $7.550 \rightarrow 6.789$ transition strengths are equal. The average $E1$

TABLE XI. Comparison of relative strengths for transitions from the N^{15} 8.312- and O^{15} 7.550-MeV levels.

J^{π} Final state	Multi-polarity	$\Gamma_{\gamma}(O^{15})$[a] (10^{-3} eV)	O^{15} transition strength (Weisskopf units)	N^{15} transition strength[b] (arbitrary units)
$\frac{1}{2}^{-}$	$E1$	1.3 ± 0.5	0.73×10^{-5}	$(0.3\pm0.05)\times10^{-2}$
$\frac{3}{2}^{-}$	$E1$	23 ± 0.5	0.022	0.03 ± 0.01
$\frac{1}{2}^{+}$	$M1$	6.7 ± 0.5	0.024	0.20 ± 0.05
$\frac{3}{2}^{+}$	$M1$	9 ± 0.5	0.97	(0.97)

[a] Assuming a total gamma-ray radiative width of 40×10^{-3} eV [S. Bashkin, R. R. Carlson, and E. B. Nelson, Phys. Rev. **99**, 107 (1955)].
[b] Normalized to the strength of the O^{15} transition to the $\frac{3}{2}^{+}$ state.

transition strength in light nuclei is about 0.055 Weisskopf units with a spread of about a factor of seven; for $M1$ transitions the average strength is about 0.15 Weisskopf units with a spread of about a factor of 20.[43] Thus, the transitions from the O^{15} 7.550-MeV level to the $J=\frac{3}{2}$ states at 6.180 and 6.789 MeV have close to normal strengths; the $M1$ transition to the 5.188-MeV level is somewhat smaller than normal and the $E1$ transition to the ground state is extremely weak. From the data given in Table XI it is clear that the transitions to the $J=\frac{3}{2}$ states in N^{15} are also the strongest (relative to the average) and that the relative strengths of these two transitions in N^{15} are consistent with those in O^{15}. For the transitions to the $J=\frac{1}{2}$ states, however, there is a gross discrepancy between O^{15} and N^{15} assuming that our normalizing assumption is roughly correct. This discrepancy probably indicates a strong effect of the Coulomb interaction which may occur because there is strong cancellation between different contributions to the dipole matrix elements in both nuclei, and slight changes in the wave functions due to the Coulomb interaction are thereby greatly magnified. This effect is probably related to the large Thomas-Ehrman[45] shift of the 7.550-MeV level which occurs due to its large s-wave nucleon reduced width and its proximity to the $N^{14}+p$ threshold.

The N^{15} 8.570- and O^{15} 8.283-MeV Levels

We find the N^{15} $8.570\rightarrow 0$ transition to be $E1$ so that the 8.570-MeV level has $J^\pi=\frac{1}{2}^+$ or $\frac{3}{2}^+$. Since $\frac{1}{2}^+$ was excluded previously,[8,9] the N^{15} 8.570-MeV level has $J^\pi=\frac{3}{2}^+$. Angular-correlation measurements on the unresolved ground-state transitions from the N^{15} 8.31- and 8.57-MeV levels have previously shown that the $E1$, $M2$ mixing ratio of the N^{15} $8.57\rightarrow 0$ transition is $x=-(0.13\pm 0.25)$ or $+(2.7\pm 1.6)$ if the N^{15} 8.31-MeV level has $J=\frac{1}{2}$. The internal-pair correlation measurement rules out the latter alternative, so that the N^{15} $8.57\rightarrow 0$ transition has $x=-(0.13\pm 0.25)$ if the N^{15} 8.31-MeV level has $J^\pi=\frac{1}{2}^+$.

The pairing of the N^{15} 8.570-MeV level with the O^{15} 8.283-MeV level seems conclusive. Both levels have $J^\pi=\frac{3}{2}^+$, the difference in excitation energies is in good agreement with the general trend, and the gamma-ray decays are also in good agreement.

The N^{15} 9.052- and O^{15} 8.735-MeV Levels

The N^{15} $9.052\rightarrow 0$ transition was found to be $E1$ so that $J^\pi=\frac{1}{2}^+$ or $\frac{3}{2}^+$ for the 9.052-MeV level. This is consistent with the $N^{14}(d,p)N^{15}$ stripping results of Sharp *et al.*[14]

The energy systematics favor a pairing of the N^{15} 9.052-MeV level with the O^{15} 8.735-MeV level. The spin-parity information (Figs. 24 and 25) is consistent with this; however, the decay modes of these two states are markedly different (Figs. 24 and 25). If we were guided by decay modes alone, we would pair the N^{15} 9.052-, 9.155-, and 9.223-MeV states with the O^{15} 8.980-, 8.915-, and 8.735-MeV states, respectively. This may, in fact, be correct; however, the pathological disagreement of the decay modes of the N^{15} 8.312-, O^{15} 7.550-MeV mirror pair cautions us against a strong reliance on comparison of gamma-ray decay modes for the purpose of pairing levels in mirror nuclei.

The N^{15} 9.223- and 9.155-MeV Levels and the O^{15} 8.980- and 8.915-MeV Levels

The N^{15} 9.223-MeV level was observed to decay to the $J^\pi=\frac{1}{2}^+$ 5.299-MeV level; no other transitions were observed. The lifetime limit, $\tau<5\times 10^{-13}$ sec, limits the spin of the 9.223-MeV level to $J\leqslant\frac{5}{2}$ since the $9.223\rightarrow 5.299$ transition cannot be of higher order than quadrupole. No other information is available for this level.

The N^{15} 9.155-MeV level has a complex decay scheme (see Fig. 24). The lifetime limit restricts the spin-parity of the 9.155-MeV level as follows: the $9.155\rightarrow 7.154$ transition cannot be $M2$ or $E3$ so that $J^\pi=\frac{1}{2}^-$ is not allowed and spins of $\frac{7}{2}$ or higher are forbidden by the transitions to the ground state, 5.299-MeV level, and 6.323-MeV level. The internal pair correlation measurement on the $9.155\rightarrow 0$ transition rules out pure $E1$ radiation so that $J^\pi=\frac{1}{2}^+$ is also ruled out. Thus, the spin of the N^{15} 9.155-MeV level is $\frac{3}{2}$ or $\frac{5}{2}$. Of the four possible spin-parity assignments $\frac{3}{2}^+$ is extremely unlikely since the $9.155\rightarrow 0$ transition would then have a strong admixture of $M2$ radiation with $E1$ radiation (Fig. 23). An assignment of $\frac{3}{2}^-$ appears the most likely, although $\frac{5}{2}$ (pure quadrupole or quadrupole-octupole mixtures for the $9.155\rightarrow 0$ transition, see Fig. 23) cannot be completely excluded.

From the energy correspondence, it appears likely that the O^{15} 8.980- and 8.915-MeV levels are the mirror levels of the N^{15} 9.223- and 9.155-MeV levels. If so, the available spin-parity information (Figs. 24 and 25) would favor an inversion of the two levels between N^{15} and O^{15}. On the other hand, a pairing of the N^{15} 9.155-MeV level and the O^{15} 8.915-MeV level is indicated by a comparison of the gamma-ray decay modes. We note that the decay modes of the N^{15} 9.223-MeV level bear little resemblance to those of either the 8.980 or the 8.915-MeV level of O^{15}. It appears that more information is necessary before a one-to-one correspondence can be established between the two N^{15} levels and the two O^{15} levels under discussion.

The N^{15} 9.929- and 9.762-MeV Levels

These two states were formed relatively weakly in the $N^{14}(d,p)N^{15}$ reaction and strongly in the $C^{14}(d,n)N^{15}$ reaction indicating considerably larger coefficients of fractional parentage for the first $(J^\pi,T)=(0^+,1)$ state of mass 14 than for the first $(1^+,0)$ state. The internal

---

[45] R. G. Thomas, Phys. Rev. 88, 1109 (1952); J. B. Ehrman, *ibid.* 81, 412 (1951).

pair measurements indicate that the ground-state transitions from both levels are $E1$ and hence $J^\pi=\frac{1}{2}^+$ of $\frac{3}{2}^+$. However, the uncertainties of the measurements are large enough to allow a possibility for $E2$ in both cases, and thus $J^\pi=\frac{3}{2}^-$ or $\frac{5}{2}^-$ cannot be excluded. For an $E1$ assignment we have $J^\pi=\frac{1}{2}^+$ or $\frac{3}{2}^+$. Either of these assignments is consistent with the gamma-ray decays (see Table V or Fig. 24) which are primarily to the ground state for both levels with some evidence of cascades from the 9.93-MeV level.

An argument in support of $J^\pi=\frac{1}{2}^+$ assignments for both N^{15} levels is the intense threshold effect (i.e., large cross section at threshold) for these levels observed by Chiba[5] using the $C^{14}(d,n)O^{15}$ reaction. This suggests[46] formation of these levels by the stripping mechanism with $l_p=0$ and thus $J^\pi=\frac{1}{2}^+$.

We note that these two levels and the 10.074-MeV level gave considerably stronger threshold effects than any others for the deuteron energy range studied by Chiba.[5]

There is no reported evidence concerning the spin-parity assignments of these two levels from the $N^{14}(d,p)N^{15}$ reaction.

The N^{15} 9.832-MeV Level

This level was observed to decay to the $J^\pi=\frac{5}{2}^+$, 5.270-MeV level. No other decay modes were observed. The state is formed weakly in $N^{14}+d$ and $C^{14}+d$ but relatively strongly in $C^{13}+He^3$. From the lifetime limit, $\tau<5\times10^{-13}$ sec, and the observed decay mode we can set a limit $J\leqslant\frac{9}{2}$ on the spin of this level with $J=\frac{3}{2}$, $\frac{5}{2}$, or $\frac{7}{2}$ preferred. There is no previous information on the spin-parity assignment of this level.

The N^{15} 10.074-MeV Level

This level is formed relatively strongly in the $N^{14}(d,p)N^{15}$ reaction (see Fig. 21) and using this reaction we obtained an unambiguous $E1$ assignment for the $10.074\to0$ transition. Therefore the 10.074-MeV level has $J^\pi=\frac{1}{2}^+$ or $\frac{3}{2}^+$. The only observed decay mode of this state is to the ground state (Table V and Fig. 24) which is reasonable for $J^\pi=\frac{1}{2}^+$ or $\frac{3}{2}^+$.

The N^{15} 10.074-MeV level has previously been studied by analyzing the angular distributions of protons following the $N^{14}(d,p)N^{15}$ reaction using plane-wave stripping theory. An assignment of $l_n=1$ resulting in $J^\pi\leqslant\frac{5}{2}^-$ (Fig. 1) was obtained from this work[14,16] in disagreement with the present result. The reason for this discrepancy may be the inadequacy of the plane wave stripping theory for a level so close to the neutron binding energy (10.834 MeV).

As was the case for the N^{15} 9.929- and 9.762-MeV levels, an assignment of $J^\pi=\frac{1}{2}^+$ is suggested by the intense threshold effect for this level in the $C^{14}(d,n)N^{15}$ reaction.[5] However, an assignment of $J=\frac{1}{2}$ is inconsistent with our observation of anisotropy for the $10.074\to0$ transition (Table I). Because of this discrepancy we retain both $J^\pi=\frac{1}{2}^+$ and $\frac{3}{2}^+$ as possibilities for this level.

Note added in proof. Angular-correlation measurements on the $C^{13}(He^3,p\gamma)N^{15}$ reaction result in an unambiguous assignment of $\frac{3}{2}^+$ for the N^{15} 10.074-MeV level and $\frac{7}{2}$ for the N^{15} 9.832-MeV level. (E. K. Warburton and J. W. Olness, to be published).

The N^{15} 10.452-MeV Level

For this virtual level we find $\Gamma_\gamma/\Gamma>0.85$, 0.7 to one and two standard deviations. Combining these limits with the branching ratios (Table V) gives $\Gamma_{\gamma0}/\Gamma>0.07$, 0.055 to one and two standard deviations, respectively. These limits are consistent with the rough estimate, $\Gamma_{\gamma0}/\Gamma\sim0.1$ made by Hebbard and Dunbar,[17] but change the results of the $C^{14}(p,\gamma)N^{15}$ analysis (Table II of Ref. 17) somewhat to give the values $\omega\Gamma_p\sim0.00025$ eV; $\omega\Gamma_\gamma\gtrsim0.0006$ eV.

The N^{15} 10.800-MeV Level

The branching ratios we obtained for this $J=\frac{3}{2}$ level (Table V and Fig. 24) are in fair agreement with the previous $C^{14}(p,\gamma)N^{15}$ results of Hebbard and Dunbar[17] and of Bartholomew *et al.*[47] We obtain $\Gamma_\gamma/\Gamma=0.55_{-0.15}^{+0.25}$ for the 10.80-MeV level, or $\Gamma_{\gamma0}/\Gamma=0.3_{-0.09}^{+0.15}$. This latter value is in good agreement with the rough estimate, $\Gamma_{\gamma0}/\Gamma\sim0.2$, made by Hebbard and Dunbar[17] so that our results do not change their analysis significantly.

B. Comparison with Theory

The Odd-Parity Levels

The two $T=\frac{1}{2}$ states arising from the shell-model configuration s^4p^{11} (also referred to as p^{-1}) have long been identified with the ground states and third-excited states of N^{15} and O^{15}. It is of interest to identify and determine the properties of higher lying odd-parity states. By doing so we can gain a greater understanding of the systematics of excited configurations in the p shell and the information can give a firmer basis from which to estimate the admixtures of these configurations in the two $T=\frac{1}{2}$, p^{-1} states.

It is apparent from inspection of Figs. 24 and 25 that there are several possible odd-parity levels in N^{15} or O^{15} below an excitation energy of 11 MeV but that not enough is known at present to identify any except the 8.980-MeV level of O^{15} and its analog in N^{15}.

From systematics in other light nuclei, it appears likely that odd-parity levels below an excitation energy of 11 MeV in N^{15} and O^{15} could arise from three configurations other than p^{-1}. These are $p^9(2s,1d)^2$,

[46] E. K. Warburton and L. F. Chase, Jr., Phys. Rev. 120, 2095 (1960).

[47] G. A. Bartholomew, F. Brown, H. E. Gove, A. E. Litherland, and E. B. Paul, Can. J. Phys. 33, 441 (1955).

$p^7(2s,1d)^4$, and $p^{10}f_{7/2}$, where $(2s,1d)^n$ refers to n nucleons in the nearly degenerate $2s_{1/2}$ and $1d_{5/2}$ shells. The first two of these configurations could give rise to several $J^\pi=\frac{1}{2}^-$ and $\frac{3}{2}^-$ states, while the lowest states of $p^{10}f_{7/2}$ would probably have $J^\pi \geqslant \frac{5}{2}^-$.

In a study of the $B^{11}(Li^6,d)N^{15}$ and $B^{11}(Li^7,t)N^{15}$ reactions, McGrath and Carlson[48] observed that the cross section for formation of the N^{15} 9.155-MeV level is about 10 times larger than that for any other N^{15} level. They conjectured that the 9.155-MeV level has $J^\pi=\frac{3}{2}^-$ and belongs predominantly to the $p^7 2s_{1/2}{}^4$ configuration. On the basis of their observations alone, however, it would appear that the less restrictive configuration $p^7(2s,1d)^4$ is as likely, as is the configuration $p^9(2s,1d)^2$.

The Even-Parity Levels

The even parity levels of N^{15} and O^{15} have been investigated theoretically by Halbert and French[49] who performed an intermediate coupling calculation assuming the configurations $s^4p^{10}2s$, $s^4p^{10}d$ and s^3p^{12}. They were able to make quite convincing correlations between theory and experiment for the 7 even-parity levels of N^{15} below an excitation energy of 9 MeV. They found that, in their model, the s^3p^{12} configuration came at a much higher energy than the $p^{10}(2s,1d)$ configuration and had very small admixtures in the lowest 7 even-parity levels.

These authors also calculated level energies and nucleon reduced widths, but only presented β- and γ-decay matrix elements in two cases: for the β decay of C^{15} to the N^{15} 5.299-MeV level and for the N^{15} $8.570 \rightarrow 0$ $E1$ transition.[50] For the C^{15} β decay they obtained a theoretical $\log ft$ value of 4.8. The experimental value[10] of 4.07 ± 0.03 is intermediate between this result and that obtained[51] assuming that the C^{15} ground state and N^{15} 5.299-MeV level are the $T=\frac{3}{2}$ and $T=\frac{1}{2}$ states obtained from coupling a $2s_{1/2}$ nucleon to the lowest $(J^\pi,T)=(0^+,1)$ level of p^{10}. For the N^{15} $8.570 \rightarrow 0$ $E1$ transition Halbert and French predicted a radiative width of 0.28 eV. The radiative width of this transition is not known but that of the mirror transition, O^{15} $8.283 \rightarrow 0$ has been measured to be 0.53 eV.[26,52] A radiative width of 0.28 eV for the N^{15} $8.570 \rightarrow 0$ transition corresponds to 0.25 eV for the O^{15} $8.283 \rightarrow 0$ transition. We consider this agreement between theory and experiment to within a factor of ~ 2 to be quite good for such a weak transition (1×10^{-3} Weisskopf units).

Halbert and French predicted that the eighth and ninth even-parity levels in N^{15} and O^{15} would have $J=\frac{9}{2}$ and $\frac{7}{2}$, respectively. Both these states would probably have negligibly small ground-state transitions, the $J=\frac{9}{2}$ level would probably cascade through the first $J=\frac{7}{2}$ state and both could have strong cascades to the first $J=\frac{5}{2}$ state. From Figs. 24 and 25 we see that the $J=\frac{9}{2}$ state is most likely above an excitation energy of 11 MeV while the N^{15} 9.83-MeV level is the only N^{15} level below an excitation energy of 11 MeV for which an identification with the $J=\frac{7}{2}$ level seems likely. Thus it would appear that the majority of the even-parity levels between 9 and 11 MeV in N^{15} arise from some configuration other than $p^{10}(2s,1d)$. One likely configuration beginning in this region of excitation is $p^8(2s,1d)^3$, for which the ordering of levels might bear some resemblance to the even-parity level spectrum of F^{19}. Unna and Talmi[53] have predicted a $(J^\pi,T)=(\frac{1}{2}^+,\frac{1}{2})$ level of $p_{3/2}{}^8 2s_{1/2}{}^3$ at an excitation energy of 7.00 MeV in N^{15}; thus it is plausible that the $p^8(2s,1d)^3$ spectrum of which this level is a member begins near an excitation of 9 MeV or lower.

It is clear that a great deal more information is desirable in order to compare fully with theory the properties of nuclear levels of mass 15. On the experimental side, the spin and parities of most of the levels between 9 and 11 MeV in N^{15} are yet to be determined. None of the lifetimes of the N^{15} levels have been determined. Lifetime measurements would be of interest for comparison with theory and also for comparison with those O^{15} lifetimes which have been determined by the $N^{14}(p,\gamma)O^{15}$ reaction. On the theoretical side, a calculation of the $\log ft$ values for the β decay of C^{15} to all the states of N^{15} which are energetically available and a calculation of gamma-ray transition strengths using the model of Halbert and French[49] or some alternative model (of equal or greater validity) would be very valuable. A theoretical question of special interest is posed with regard to the very large difference between the gamma-ray transition strengths for the decays of the N^{15} 8.312- and O^{15} 7.550-MeV levels. For instance, how is this difference related to the large Thomas-Ehrman shift of the O^{15} 8.550-MeV level?

ACKNOWLEDGMENTS

We wish to thank C. Chasman and R. A. Ristinen for the loan of the Li-Ge detector, and K. W. Jones for his advice and assistance in its use. H. T. Motz, B. Povh, W. Scholz, J. B. Marion, A. E. Evans, A. Gallmann, and E. Kashy are to be thanked for communications concerning their unpublished work, while J. N. McGruer and L. F. Chase, Jr. very kindly supplied us with enriched carbon targets.

[48] R. L. McGrath and R. R. Carlson, Bull. Am. Phys. Soc. **10**, 443 (1965).
[49] E. C. Halbert and J. B. French, Phys. Rev. **105**, 1563 (1957).
[50] However, J. B. French and S. Iwao (unpublished) have used the Halbert and French (Ref. 49) wave functions to calculate the $\log ft$ values for the β decay of C^{15} to the first $J^\pi=\frac{3}{2}^+$ and second $J^\pi=\frac{1}{2}^+$ states of N^{15} (see Table IV of Ref. 10).
[51] See footnote 47 of Ref. 29.
[52] D. B. Duncan and J. E. Perry, Phys. Rev. **82**, 809 (1951).
[53] I. Unna and I. Talmi, Phys. Rev. **112**, 452 (1958).